Characterization of coating on graphite anode material for lithium-ion batteries

JØRGEN GRIMENES

SUPERVISORS
Gunstein Skomedal
Bernhard Fäßler
Peter Huge Middleton

University of Agder, [2021]
Faculty of Engineering and Science
Department of Engineering Sciences

Abstract

To improve the performance of lithium-ion batteries, the graphite anode can be treated with special coating. Thus the charge transfer resistance through the material can be lowered and thereby enable e.g. faster charging. The amount of coating is essential the improve the performance. The thesis is investigating thermogravimetric and electrochemical impedance spectroscopy as a method to identify an optimal relation between the amount of coating and the charge transfer resistance.

There is found that lower material resistivity gives a higher weight loss where it is assumed that the coating is oxidising, methods for both a relative difference in the weight loss and direct measurement of the weight loss was develop. There was fund a connection between the charge transfer resistance and the resistivity as well. There were too few samples to conclude which method works best or make a firm conclusion of the methods. To further improve the developed methods, there should be more standardised tests with wider varieties of samples in each category. A more developed method should also be used to check if the result is correct.

Preface

Before starting on the master thesis, I have taken a bachelor in renewable energy at the University of Agder. This was so interesting that I applied for a master's degree in renewable energy at the same university instead of start working. Renewable energy is a large field with many directions to take. Still, one of the most exciting and fastest developments is in batteries and, more specific lithium-ion battery. Since I believe it will be a critical part of the future energy system, did I choose to work more with this when I should do my master thesis. I was lucky to be able to do this in collaboration with Elkem carbon. This has given me a chance to do a thesis in close connection with the industry. In that context, I wish to thank Navaneethan Muthuswamy that work at Elkem, for support with the thesis. I also like to thank Odin Kvam for his good support with the thermogravimetric experiments. And I will like to thanks the supervisors Gunstein Skomedal, Bernhard Fäßler and Peter Huge Middleton.

Individual/group Mandatory Declaration

The individual student or group of students is responsible for the use of legal tools, guidelines for using these and rules on source usage. The statement will make the students aware of their responsibilities and the consequences of cheating. Missing statement does not release students from their responsibility.

1.	I/We hereby declare that my/our report is my/our own work and that I/We have not used any other sources or have received any other help than mentioned in the thesis.	☒
2.	I/we further declare that this thesis: - has not been used for another exam at another department/university/university college in Norway or abroad; - does not refer to the work of others without it being stated; - does not refer to own previous work without it being stated; - have all the references given in the literature list; - is not a copy, duplicate or copy of another's work or manuscript.	☒
3.	I/we am/are aware that violation of the above is regarded as cheating and may result in cancellation of exams and exclusion from universities and colleges in Norway, see Universitets- og høgskoleloven §§4-7 og 4-8 og Forskrift om eksamen §§ 31.	☒
4.	I/we am/are aware that all submitted theses may be checked for plagiarism.	☒
5.	I/we am/are aware that the University of Agder will deal with all cases where there is suspicion of cheating according to the university's guidelines for dealing with cases of cheating.	☒
6.	I/we have incorporated the rules and guidelines in the use of sources and references on the library's web pages.	☒

Publishing Agreement

Authorization for electronic publishing of the thesis.

Author(s) have copyrights of the thesis. This means, among other things, the exclusive right to make the work available to the general public (Åndsverkloven. §2).

All theses that fulfill the criteria will be registered and published in Brage Aura and on UiA's web pages with author's approval.

Theses that are not public or are confidential will not be published.

I hereby give the University of Agder a free right to

make the task available for electronic publishing: ☒JA ☐NEI

Is the thesis confidential? ☐JA ☒NEI

(confidential agreement must be completed and signed by the Head of the Department)

- If yes:

Can the thesis be published when the confidentiality period is over? ☐JA ☐NEI

Is the task except for public disclosure? ☐JA ☒NEI

(contains confidential information. see Offl. §13/Fvl. §13)

Table of Contents

List of Figures

List of Tables

Notation

A =	area
$°C$ =	Degree Celsius
C =	capacitance
$C_{electrod}$ =	Electrode capacitance
C_{SEI} =	SEI-layer capacitance
g =	gram
h =	height
I =	current
mL =	millilitres
L =	induction
Ω =	ohm
ω =	Angular frequency
$\mu\Omega$ =	micro-ohm
m =	meter
R =	resistance
R_b =	Bulk resistance
R_{ct} =	Charge transfer resistance
r =	Resistivity
V =	voltage
R_{SEI} =	SEI-layer resistance
Z =	impedance
W =	Warburg impedance

Abbreviations

AC = Alternating current
C = C-rate
CC = Constant current
CCCV = Constant current-constant voltage
CO2 = Carbon dioxide
CV = Constant voltage
DSC = Differential scanning calorimetry
DoD = Depth of discharge
DC = Direct current
E = Potential
LTO = Lithium titanate
N2 = Nitrogen
Nm = nanometre
O2 = Oxygen
PC = Propylene carbonate
TEM = Transmission electron microscopy
TGA = Thermogravimetric analysis
Tr = Reference temperature
Ts = Sample temperature
Tc = cell temperature
SoH = State of health
UiA = University of Agder
Nm = nanometre
Wt = weight

1. Introduction

With increased attention to contamination and global warming, there is an increased interest in electrification to make a renewable society. Some increase in renewable energy can substitute electric power already used in the grid produced for non-renewable sources. However, electrification of arias that earlier have used fossil energy for transportation is also necessary to go beyond that. Except for some cases as electric trains, subways and trams, most transportation has taken place with petroleum products as fuel because of the necessities to transport the fuel. To electrify the rest of the transport sector with renewable energy, there is a need to store the electric power and transport it with the vehicle, ship, or plane.

There is a need for better batteries to achieve this, better in many ways like capacity, energy density, better safety, more renewable material and reuse. However, an improvement that is especially important for electrification of transportation like cars, trucks, small bot, and more, is the charge rate, to charge the battery or at least a proportion of it in a short time. One of the challenges with this is to get the lithium ions into the anode material fast enough when using graphite as an anode.

The primary work method for this thesis is to perform a series of experiment, and evaluation of them along the way, to develop a method for characterization of carbon coating on graphite. The process is going to be supported by theory and literature.

Project name:
Characterization of coating on graphite anode material for lithium-ion batteries

To improve lithium-ion batteries charging and discharging performance, one method is to use a coating. Thus, it is essential to use the right amount of coating, both for the cost of production and the best effect. In this thesis, there is looked at the problem of quantifying the amount of coating used in a graphite sample, either by looking at the sample or at a battery where the anode is made with this sample.

2. Theory

2.1 Batteries

Batteries describe a type of electrochemical energy storage units. There are a lot of different variations of batteries that differ in size, material, and structure. This allows having batteries with different parameters, performance, and applications. The development of batteries has been ongoing for hundreds of years. Some traces can already be found back in BC time [1]. However, the development of the electrochemical cell, as we know it today, started in the eighteenth century with the research activities of Galvani and Volta. Volta made a pilar with silver and zinc discs that could generate electricity. In 1859 the French scientist Gaston Plante invented a rechargeable battery, the lead-acid battery.[1]

There are many ways to categorize batteries, but they are usually categorized in three main groups each with a lot of sub-groups. Consisting of primary, secondary, and fuel cells. Primary batteries are the first developed type of batteries. This type of battery with an irreversible reaction cannot be recharged. Thus, they are single use. An early example is the Daniell Element, developed in 1836.

Secondary batteries are batteries that can be recharged and used multiple times. This happens by applying an external electric force opposite to the electrochemical process. Thereby the electrochemical process is reversed and take its original form. How many times this can be done before is the battery reaches its end of life dependent on the battery chemistry and others factor as charging power, depth of discharge, temperature, use pattern, and time. There are some clear advantages with the use of secondary batteries. They are economically favourable if it is used enough times to overcome the extra cost. Thus, it is also much more environment friendly and for many applications with integrated batteries it is easier to recharge than to change the batteries.
There are four normal shapes of cells, and they come many in different sizes. Cylindrical cells as the name indicate are formed as a cylinder and the electrodes are wrapped in layers with the separator around the middle of the cylinder. Button-cells are flat and circular cells, and easy to build. Prismatic cells also use a wrapping of different layers around the middle of the cell. This makes a compact cell that is much used in mobile phones and laptops. Pouch cells are a design that uses flexible frame material that allows it to swell more than other types and give a high packaging efficiency. Battery cells can be combined into different forms of modules and packs, where it often also includes a battery management system to control the unit and have more individual control of the cells. [2]

There is also a wide range of different voltage to choose from depending on the battery chemistry and cell/module combinations. For flow batteries and fuel cell the size will be somewhat unclear since it composes of a sperate “fuel” unit. [1][3]

2.1.1 Working principal

A battery cell generates electric power from a chemical reaction. The cell consists of two electrodes, the anode and the cathode, with different potential which are dipped into an

electrolyte and separated by a separator. If there is a metal A and B where B is nobler than A and they are dipped in an electrolyte solution that partly dissolves both metals an electron density will build up. Since the potential on the metal is different, there will also be a difference in the electron density of the two sides. If the two electrodes are connected with a conductor, the electrons will flow from the side with the highest density to the side with lower density until the energy density is equal on both sides. This will result in more dissolving of metal A to A^+ an e^- where the e^- will keep on going the B side.

$$A \rightarrow A^+ + e^- \qquad \text{Eq.1}$$

On the positive electrode side, the current received result in a higher electron density. This will be compensated for by the consumption of more electrons for the deposit of B^+.

$$B^+ + e^- = B \qquad \text{Eq.2}$$

This process will go on until metal A is fully dissolved or there is no more B+ ions. To have enough B+ ions, the electrolyte solution needs to contain B^+ ions while the separator needs to prevents them from crossing over to the A side.[3]

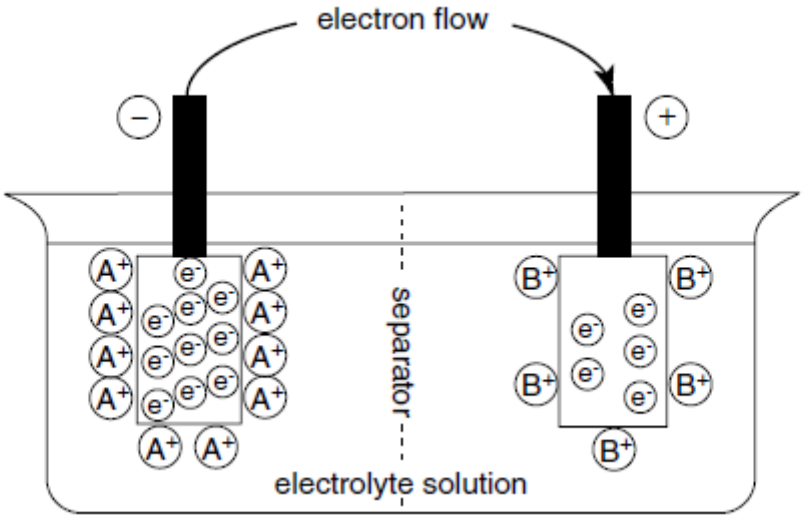

Figure 1 Basic work principle [3]

2.1.2 Terminal voltage

The terminal voltage, also called potential, is the voltage difference between the anode and cathode of the battery. The theoretical terminal open circuit potential depends on the potential difference of the metals used in the electrodes. The potential of the materials can be found in the electrochemical series.

The potential of a material is usually measured against the potential of hydrogen under standard conditions, defined as zero and the other material will then be placed on the positive or negative axis with the difference from hydrogens potential as value. There is

also sometimes used a different scale where Li/Li+ is defined as zero, this scale will almost only be on the positive side since Li/Li+ has a low potential. The equating for the cell potential is shown in eq. 3, where $E^0_{positive}$ and $E^0_{negative}$ is the standard electrode potential for the different materials [3]

$$E^0_{cell} = E^0_{positive} - E^0_{negative} \quad \text{Eq.3}$$

2.1.3 C-rate

The C-rate is a number that tells the charging or discharging ability of a battery based on its rated capacity. It can be calculated according to eq. 4 where rated capacity is in amper per hour and current in ampere. The rate of 1 C corresponds to charging or discharge the rated capacity in one hour, while a C-rate of 2 C corresponds to charging or discharge the rated capacity in half an hour. Parameters as lifetime, total capacity, and voltage can depend on the C-rate. This makes it an important parameter when working with and comparing battery. [3]

$$C = \frac{Charge\ or\ discharge\ current}{Rated\ capacity} \quad \text{Eq.4}$$

2.1.4 State of health

The state of health (SoH) is the battery's actual capacity compared to the initial rated capacity. There will always be ageing in a battery over time and use that degenerate the battery. To show this, the SoH is a useful parameter. Many applications have a SoH minimum level. This can be used to give an estimate of the lifetime to the battery, where typically it shall be able to achieve a specific number of cycles before it goes below a certain SoH level.[3]

$$SoH = \frac{Usabel\ capacity}{Rated\ capacity} \quad \text{Eq.5}$$

2.1.5 State of charge and depth of discharge

The state of charge (SoC) measures the charge level of a battery, either based on its rated capacity or its actual capacity. The depth of discharge (DoD) is the reverse SoC. Low or high SoCs can harm the battery. Therefore, the minimum and maximum allowed SoC can limit the useable SoC.

$$SoC = \frac{Energy\ in\ battery}{Rated\ capacity} \quad \text{Eq.6}$$

$$DoD = 1 - SoC \quad \text{Eq.7}$$

Since it is not possible to measure the SoC directly, it must be calculated from other values. There are some methods where different battery parameters can be directly measured or compare with known values to estimate the SoC. The open circuit voltage and terminal voltage method is easy to measure but the accuracy of SoC estimation is not high. The electrochemical impedance spectroscopy method is used to detect the change in internal battery resistance. Thereby, the impedance of the battery is compared to known impedances of the battery at different SoC levels. Further, different methods have been

developed that use artificial intelligence and algorithms, like Kalman filter, support vector machine, and neural network. [4]
The method used in this work is coulomb counting, with eq. 8. The method works by measuring the current and integrate it over time. Thus, the SoC can be estimated if the initial SoC value is known, or the battery is completely charged, or discharge, and the rated capacity has been calculated. This method can still have some error since there is some self-discharge and losses change in the voltage level in the process.[4]

$$SoC(t) = SoC_0 \pm \int_{t_0}^{t_1} I_t\,(t)dt \qquad \text{Eq.8}$$

Where:
$SoC_i = Initial\ SoC\ value$
$t = Time$
$I_t = Current$
$t_0 = Start\ time$
$t_1 = End\ time$

2.2 Lithium-ion battery

The rechargeable lithium-ion battery has an abrupt growth since the first commercial production stated in 1991 by Sony. The development of the use of lithium started already in the 1950's After the first commercialization, lithium-ion batteries have had remarkable success and are now used in many applications such as computers, cell phones, and hobby drones. Larger lithium-ion battery packs are used in electric cars, buses, and backup power systems, where especially vehicles have increased the demand a lot in the last decade. And stands for around 50 % of the use in 2018.[5]. The advantages of lithium-ion batteries are a combination of lightweight and high energy density. This makes them suitable for use in application where size is essential. The lightweight also makes them useful for aerospace applications. There are some experiments with the use of lithium-ion battery in aircraft. A problem with the use of batteries in mobile applications is the currently low specific energy that is limiting travel distances. This problem will hopefully be solved with newer generations of lithium-ion batteries with higher energy densities and a strong decrease in price. The general working principles of a lithium-ion battery does not differ much from other secondary battery. The difference lies in the active materials used in the cathode, anode, and electrolyte. The name indicates that lithium is a part of the battery, combined with other materials. Some examples are lithium cobalt oxide (LiCoO2) and lithium iron phosphate (LiFePO4) in the 4-volt category. [6]

2.2.1 Specific capacity

The specific capacity is the capacity that can be stored related to units of mass. This depends on which type of material is used in the cell or battery. It can also be used specifically about the cathode or anode instead of the whole cell or battery. For lithium batteries, the specific capacity in the anode and cathode can differ a lot after which material is used. In the anode, much-used material like graphite has a theoretical capacity of 372 mAh/g, while experimental types of material like silicon can have a capacity of around ten-time higher. Also, in the cathode, there is a wide range of different materials to choose from. Thus the difference is not so significant and mostly below 200 mAh/g, while some experimental materials theoretical reach 458 mAh/g.[7]

2.2.2 Energy density

The energy is the stored energy related to the volume, and this can also be used about capacity, as volumetric capacity. This is an important parameter when the battery shall be used in applications where minimizing the use of space is essential, like cell phones.[3]

2.2.3 Internal resistance

The internal resistance in a battery is the opposition of the flow of current. It composes of two different resistance, the electronic resistance, and the ionic resistance. Where the electronic resistance is the resistance that comes from the materials the battery is made of and how good the contact between them is. While the ionic resistance is the total resistance in a battery between the terminals. This is an important parameter when a battery is evaluated because it limits the specific power. Under a high current, the energy efficiency and heat are also mainly a result of the internal resistance.
[8][9]

2.2.4 Cathode

The cathode in a lithium battery needs to be able to receive, store and release ions. Finding a good cathode material is not easy, and there are many things to consider. First, it must have a sufficient specific capacity and energy density. It must endure many charged and discharge cycle at an acceptable speed. These parameters must be combined with high safety and low price. There is still not a material that gives a perfect combination of this. Therefore, some compromise must be made. There is much research going on to solve the different challenges. The different cathode materials can be categorized into two main categories. The intercalation category uses the principle of intercalation. And the conversion category, where the material undergoes a solid-state redox reaction during the insertion and depletion of the lithium ions. In each group, there is different subgroups and types. One type in the intercalation group is lithium cobalt dioxide. This was the first material used in the rechargeable lithium-ion battery and is still much used. It has a high theoretical specific capacity of 274 [mA h/g]. On the downside, its performance is strongly affected by thermal instability and its structure instabilities at high voltage. It is also expensive because of the cobalt used. This has been tried to improve by different coatings consisting of different materials. [7][5]

2.2.5 Anode

Pure lithium as an anode has a very high specific capacity and a very low potential that results in a high cell voltage. It is not much used because lithium metal will produce dendrites that can destroy the separator layer and thus cause a short circuit. It does also have a bad cycle lifetime. Therefore, a material that can hold lithium-ion is used instead, this usually gives a lower specific capacity, but make it safer and give longer-lived cell. Much work is ongoing to improve lithium metal cells using solid-state electrolytes, but it is still a cost and cycle life issues. Several different materials can be used to store lithium ions by intercalation. Graphite is most used and will be discussed in the next chapter. Amorphous carbon is an alternative that has improved safety and can deliver higher power and energy density. There is also used silicon which has a very high theoretical specific capacity of 4212 mAh/g. One of the problems with that solution is an extreme change in the volume of the material. Lithium titanate (LTO) is also used. It does not form a solid electrolyte interphase (SEI) layer, has a low cell impedance, and can reach a

capacity of 160 mAh/g. LTO thus have good cycling stability and high safety, however at the cost of lower energy density. [10] [5]

2.2.6 Button-cells

button-cells, also called coins-cell, are relatively small and flat batteries, that are easy to make and therefor a good choice when testing electrode material. A drawback is the charge and discharge time which is longer than for many other types of batteries. Typical format is 2032 (20mm diameter, 3.2mm height). For component and material testing purposes, so called "half cells" are made by replacing either the anode or the cathode with pure lithium foil as a counter electrode. When testing anode materials this means that the half cell is made of a anode electrode and a lithium foil on the other side of the separator. The anode material is now turned in to a cathode in the half cell, and the polarity of the cell is effectively reversed as compared to a standard li-ion cell.

2.2.7 Pat-cells

Pat-cells are cells where the cell part looks like the one used in a button-cell. But it is in a test module instead of a normal button-cell. There are five connections to it, one for each electrode and sensors connections for each electrode, and there is a reference connection. This makes it possible to measure the actual potential of each electrode and not just the net potential difference as in a normal coin cell / half cell. With the use of this, it is possible to measure only one of the electrodes. To hold the cells together, a specific mechanism is used that tightens precisely the cells together and makes sure that the same pressure is applied to each cell.

2.2.8 Charge discharge

There are normally three ways to control the charge or discharge of a battery. One way is the constant voltage (CV) method where a constant potential is applied, and the current will depending on the potential difference. The second method is the constant current (CC) method. Here, a chosen current is applied to the battery while the voltage will adapt. These methods (CC and CV) can also be combined to the constant-current constant-voltage (CCCV) method where the methods change based on the battery state such as the SoC.

2.3 Carbon

Carbon is element number six. It has tree know isotopes C12, C13, C14, where the first stands for 98.9 %. It has an atomic weight of 12.011. It is used as the standard for atomic mass carbon coms in many different structures, where two a seen as perfect structure, diamonds and graphite. While diamonds are the hardest know material and have a 3-d structure of sigma bonds, this also gives it very little conductivity.

2.3.1 Graphite

Graphite is a form of carbon that has a particular structure. Here, the carbon atoms are in hexagon forms in the horizontal layers and are connected with double covalent bonds and, therefore, both pi-bond and sigma-bods. While they in the vertical direction is connected with Van der Waal bonds. This makes it strongly connected in the horizon plan but weak in the vertical plane. Since the layers are so bad connected, the material can be soft and can be used as lubrication. It also gives the advantage that the material can expand in the

vertical direction, which happens when used in a lithium battery. Graphite comes with two different layers of structure. An A.B.A.B structure gives a hexagonal unit cell also called alpha, and there is an A.B.C.A.B.C structure that gives a rhombohedral stacking, also called beta. Graphite has the property to conduct electricity, because the bonds allow a delocalization of the carbon atoms in the pi-bond. Since it is the pi-bond that give the conductivity it will not work in the vertical direction where it is Van dee Waals bonds. As a result of this the resistivity can be up to 10000 time as higher in the vertical direction.[11] [12][13]

2.3.2 Types of graphite

Natural graphite is found in many places in the world it. It has many of the same properties as synthetic graphite. One main difference is that there is often a combination of hexagonal and rhombohedral form, where the last can count for up to 40 %. The rhombohedral form will only exist in natural graphite because it changes to hexagonal from at 2400 K, so it disappears in synthetic graphite. This process is irreversible. However, it is possible to make rhombohedral graphite by grinding it. Natural graphite com in three forms flake, crystalline and amorphous. The two first type have almost 100 % graphitization, while the amorphous only have 28%. [11][14]

As an alternative to natural graphite, synthetic graphite, also called artificial graphite, can be used. This is made from petroleum coke, coal-tar pitch or oil, through a heat treatment called graphitizing. The two types of graphite have different properties. Each type has polycrystalline particle and is composed of numerous single-crystalline domains. In synthetic graphite, this domain is randomly oriented, but they are orientated in the same direction in natural graphite. There is a price difference between the types, the graphitization process can last for several days, and the process demands much heat in "*The success story of graphite as a lithium-ion anode material-fundamentals, remaining challenges, and recent developments including silicon (oxide) composites*"[15] They operate with 8US$ for the natural graphite and 13US$ for the synthetic. Synthetic graphite has some benefits. It has high purity, lower thermal expansion and better thermal stability. A more isotropic orientation of the crystalline domain in each particle gives better kinetic in the intercalation process. On the downside, it has a lower capacity than natural graphite. Natural graphite has a high specific capacity but a slower charge and discharge time. This is illustrated in Figure 2. [15][13]

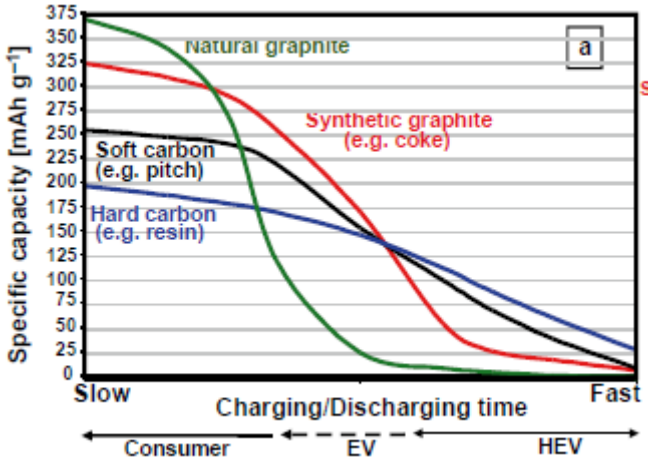

Figure 2 Illustenren of natural vs. synthetic graphite [16, p. 51]

2.3.3 Graphitising

The process of graphitising is a solid-state heat treatment of amorphous carbon materiel to make it into graphite. This happens gradually, with the increase in temperature, this process removes defect and make larger, ordered layers. Figure 3 shows how it goes from amorphous carbon at 800 degrees Celsius and to graphite around 2400 degrees Celsius. This process is not possible for all carbon types but works for the petroleum pitch, coal-tar pitch, and some coals products. These graphitisible carbons are often termed soft carbons, in contrast with non-graphitisable carbons like bio-carbon, which are forms of hard carbons. This is necessary because carbon is often in an isotropic form where the layers have a small size. The layers are not bent or twisted in some way. There can also miss some carbon atoms from the hexagonal structure, or it can be atoms from other material in the structure. The process changes the form of the material and with it its characteristics. [13][10]

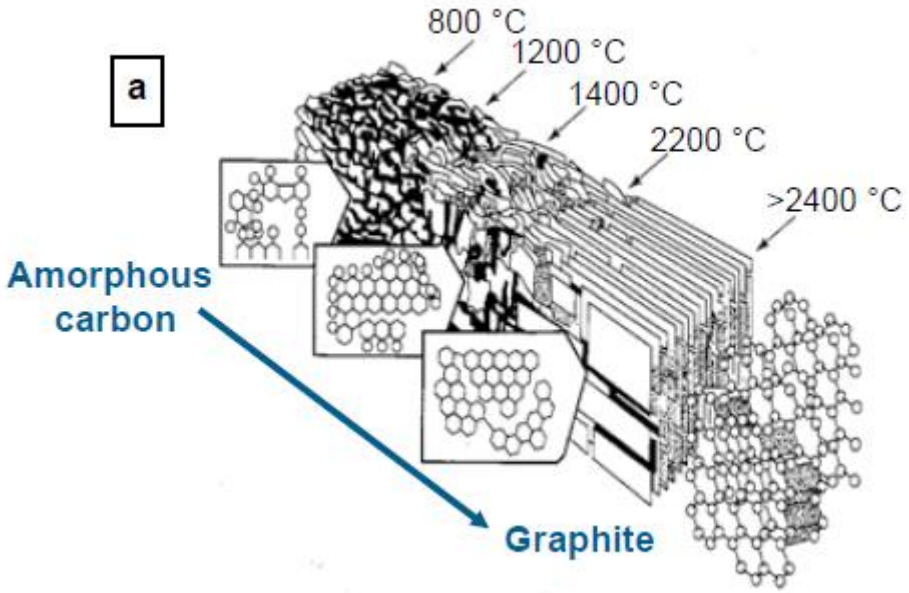

Figure 3 Graphitising of carbon[10, p. 47]

2.3.4 Intercalation

Intercalation is a process where ions are inserted between the layers in the graphite. The intercalation process needs to expand the Van der Waals bonding between the layers by approximate 10 per cent. This requires some energy and time and will therefore affect the charging rate. The intercalation of lithium ions in graphite can be divided into four stages where the number of the stages tells how many layers of graphite there are for each layer of lithium ions. There can also be included two liquid manners like stages, one before reaching stage 4 and one before reaching stage 2. Here the lithium ions are not perfectly ordered inside the layers. Each stage has a different potential related to the Li/Li^+ potential that is between 0.25 V and 0.01 V [16]

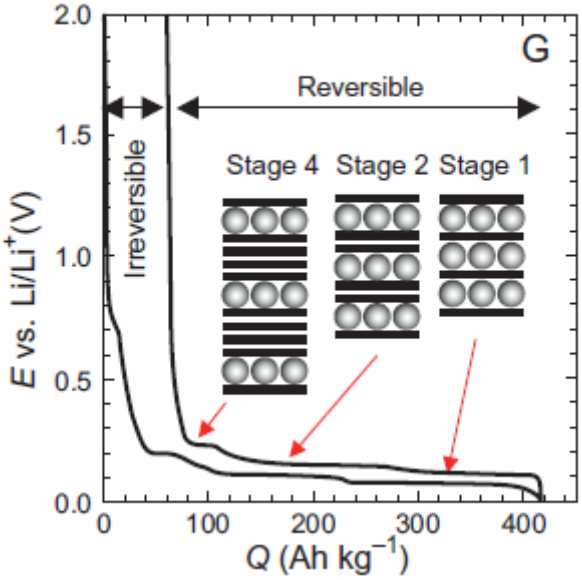

Figure 4: Intercalation stages of lithium ions in graphite [16, p. 63]

2.3.5 Types of coting

There is a variety of different types of coating that can be used. Here some are of them used on the negative electrode, shortly explained or just named. Propylene carbonate (PC) is a very good conductor and has a low melting point at -55 degrees Celsius. It is unfortunate it can not be used on graphite since it generates exfoliation and destroys the anode. But the is others alternatives to look at, like coating with carbonaceous materials. This coating has a number of positive effects. It is the first material to try and suppress the irreversible intercalation of solvent species and side reactions that come with the formation of the SEI layer. A disorientated coke shell can improve the rate of lithium ions diffusion and ensure higher capacity than graphite anode without coating. There is also much research on the use of pyrolytic carbon as a coating. This can reduce the surface area and then reduce the irreversible capacity. There is also tried different metals a coting, with the use of physical vapour deposition. There can also be used different metal oxides as a coating. [17]

2.3.6 Combustion of carbon

There is done some earlier experiment on coated graphite, in a paper from *Park, Yoon Tae Kyu Hong, YoungLee, Ki Tae* [18] they used natural graphite coated with amorphous carbon, sucrose is used. They use two samples with coating, one with 1.2 g glucose and one with 2.4 g in the mix to make coated graphite, and there is also used a sample without coating. The results show a clear difference in the Thermogravimetric analysis (TGA) and differential scanning calorimetry (DCS) profile between the samples. They calculates from the DCS profile that it is 1.3% and 3.7 % coating on the samples. There is a peak in the DCS profile and a weight loss in the TGA profile before the primary reaction. This small peak only exists in the coated samples. These peaks also have their maximum points at different temperatures, where the 1.2 g sample have it at 535 degrees Celsius, and the 2.4 sample have it at 548 degrees Celsius. There is also done transmission electron microscopy (TEM) measurement to find the thickness of the coating layer, and it is 5 and 9 nm, respectively. [18]

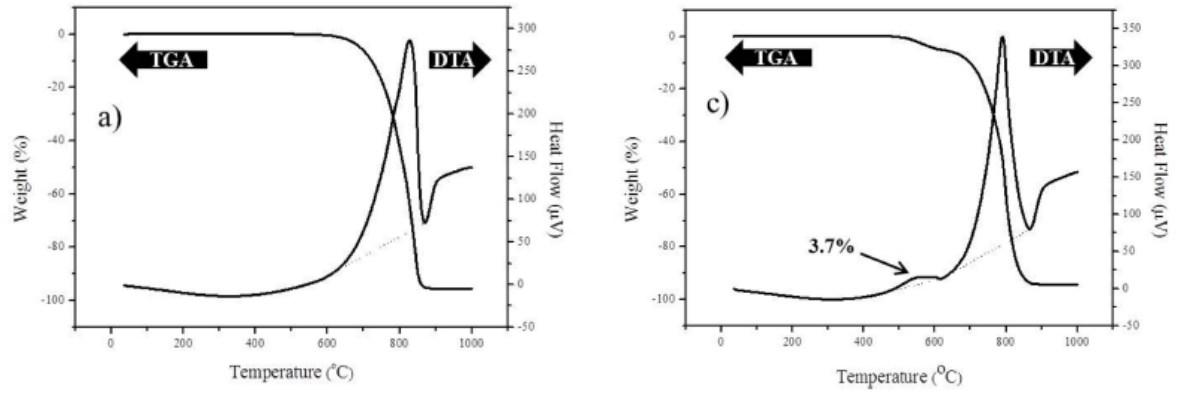

Figure 5 TGA of coated graphite [18]

Another technique used in "*Synthesis and characterization of carbon-coated LiNi13Co13Mn13O2 cathode material prepared by polyvinyl alcohol pyrolysis route - Guo al et.*"[19] measures the difference between a coated sample and an uncoated reference sample at 400 degree Celsius. It is illustrate in Figure 6 , Measurement of coating with TGA, there can also be seen that the weight difference does not change much between 400 and 500 degrees Celsius. This is done on a cathode materiel, but as a coating measurement technique it is also interesting for anode materials

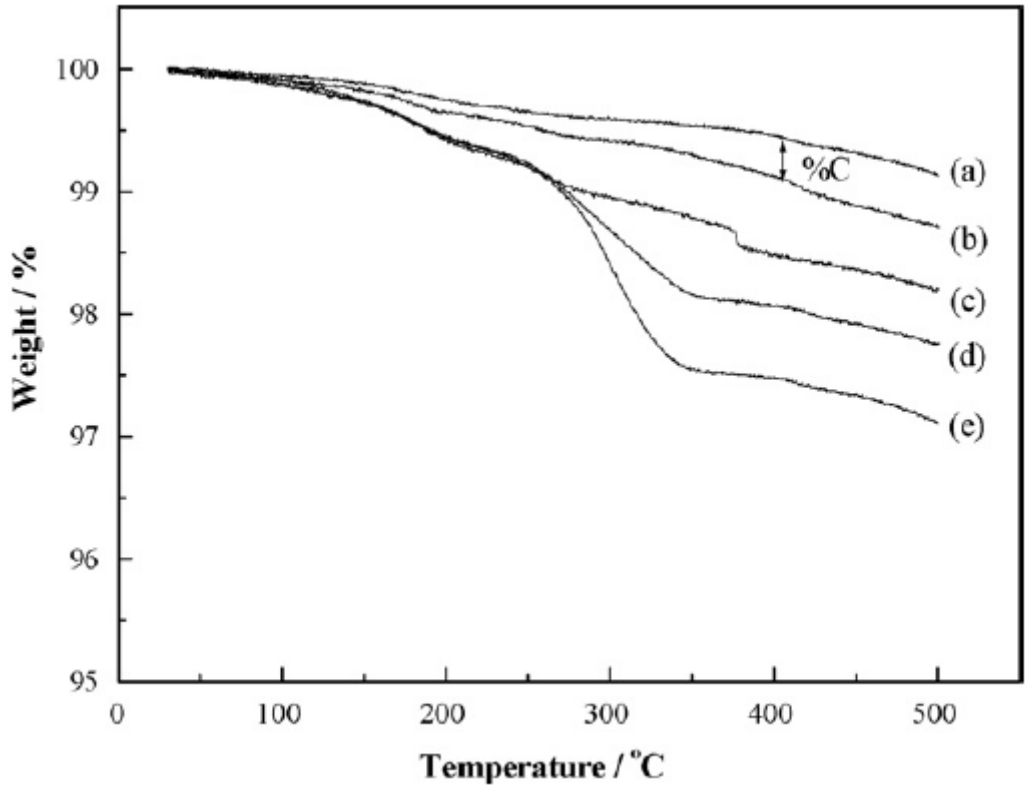

Figure 6 Measurement of coating with TGA[19]

2.3.7 Electric conductivity of carbon

The electric conductivity measure how easy a current can go through the material. It is reciprocal with resistance, which measures how much resistance the material gives the

current that goes through. This will give an important indication of how the material will work as an anode in a battery. To measure the resistance of graphite powder, it is necessary to have it in some container. Then it can be connected wires on two sides or top and bottom, where current and voltage can be applied and measured. This can be done in different ways. In the example of a setup shown in Figure 7 a cylindrical form is used, where the sample lies in a glass cylinder. The cylindrical form does not give any corners and makes it easy to compress the powder to the desired density. The pressure and density used will have a decisive impact on the result of the measurement. It is therefore important that this is the same for all samples that are compared.[20] The equation for calculating the resistivity of the material with this method is shown in Eq 9. Where r is the resistivity, V is the voltage, I the current passing through the material, A is the cross-section area, and h is the height.

$$r = \frac{V * A}{I * h} \qquad \text{Eq.9}$$

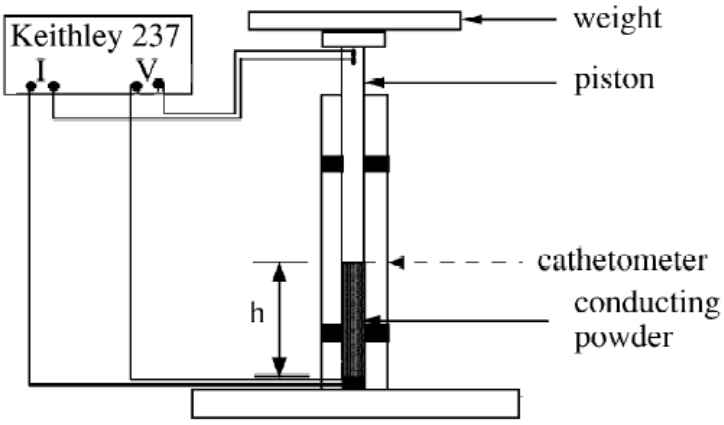

Figure 7 Resistivity measurement method [20]

2.3.8 Thermogravimetric analysis

Thermogravimetric analysis (TGA) is a method to analyse materials with the help of weight and temperature changes. The weight change that occurs with a temperature or change in temperature will give information about the material thermal stability, and the fraction of the volatile substance can be determined. There is also measured the heat flux of the material, and that is called differential scanning calorimetry (DSC).

2.4 EIS

2.4.1 Electrochemical impedance spectroscopy

Electrochemical impedance spectroscopy (EIS) is a method used to inspect a wide range thins, it is a relative new method, it has been used to analyse corrosion, catalyst, fuel cell, supercapacitor and more. It is also mare used to analyses lithium batteries.[21] One of important benefits of EIS it the ability to study different part inside an object, e.g. A battery where different efficient happing inside the different the parts, with EIS the effect to the different part can be identified and studied.

2.4.2 Working Principe

The EIS works by measuring resistance, capacity and inductance. This is done by conducting an AC voltage through the object that is investigating. Then the current response of the voltage is measured. A DC voltage will only give the real part of the impedance, and therefore just the part that usually is called the resistance and can be expressed as Eq. 10. Both parts of the impedance, real and imaginary, are shown with an AC voltage. And the frequency is also taken into the equation, shown in Eq. 11, where ω=2πf and f is the frequency. There are applied a base DC voltage and small AC voltage on top of it. The impedance will then be the interruption caused by the AC current. It is also important to note that a voltage can be used instead of current and then measure the current.

$$R = \frac{V}{I} \quad \text{Eq.10}$$

$$Z(\omega) = \frac{V(\omega)}{I(\omega)} \quad \text{Eq.11}$$

This measurement is then done on a range of different frequencies and, each frequency gives a different impedance value as long as the object includes some part that works as capacitance and /or inductance. Since the effect a capacitator or inductor will give is dependent on the angular frequency, that is dependent on the frequency, will different frequencies give different levels of impedance. When the frequency goes toward infinity, the impedance goes to zero, and when the frequency goes to zero, it will work as a DC, and therefore, do not produce any impedance. This will, in a parallel R-C circuit, give a semi-circle. A overview of the most used elements is given Table 1, and in the next chapter there effect is describe in more details [21][22]

Table 1 Equivalent circuit elements

Element	Effect	Formula AC impedance
Resistor	Resistance	R
Capacitor	Capacitance	$\frac{1}{j\omega C}$
Inductor	Inductance	$j\omega L$
Warburg	Capacitance*	$\sigma\omega^{-\frac{1}{2}} - j\sigma\omega^{-\frac{1}{2}}$
Constant phase	Capacitance*	$\frac{1}{Q(j\omega)^{\alpha}}$
Where: $\boldsymbol{R}$ = $\boldsymbol{j}$ = $\boldsymbol{\omega}$ = $\boldsymbol{C}$ = $\boldsymbol{L}$ = $\boldsymbol{\sigma}$ = $\boldsymbol{\alpha}$ = **Q =** ***=**	resistance Imaginary unit Angular frequency Capacitance Inductance Warburg coefficient Constant phase exponent parameter related to the electrode capacitance special case	

2.4.3 Equivalent circuit elements

An equivalent circuit model can mathematically model the battery cell behaviour. Such a model consists of different electrical components such as resistors, capacities, and inductances. The combination of different electrical components allows for imitating the battery behaviour. The accuracy of the model can be adjusted by the number of components used; the more components, the more accurate, but high computational power is needed, and it is harder to identify which part of battery cell the different components represent. There is some different equivalent circuit they are used in the literature, in "*Modeling and applications of electrochemical impedance spectroscopy (EIS) for lithium-ion batteries*"[21] and "*EIS study on the formation of solid electrolyte interface in Li-ion battery*"[23] is it used a Warburg in series with a resistance in R-C parallel. While in "*Micro-spherical sulfur/graphene oxide composite via spray drying for high performance lithium sulfur batteries*"[24] they use a Warburg after the last R-C-parallel

To explain how an equivalent circuit for a battery can be structured, each part is gone through step by step. It is here used a half cell system.

The simplest component used is the resistor, measured in ohm Ω. It only works in the real direction and thus has non phase shifting effect. It is named with a R.
The capacitator allows for imaginary reactive impedance Eq. 12 It has a phase-shifting effect. It is named with a C in Figure 8, the result for using the R-C in series shown in Figure 9 it does not follow the graph at all. If there instead is added at capacitor in parallel with a resistor, shown in Figure 10: R-C in parallel, the resolute is a semicircle it can be seen in Figure 11:R-C in parallel

$$Z_C = \frac{1}{j\omega C} \qquad Eq.12$$

Where ω is the Angular frequency and C is the capacitance and j it the imaginary unit, Z is the impedance.

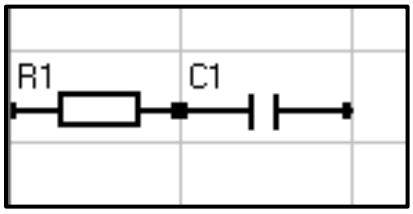

Figure 8:R-C in series

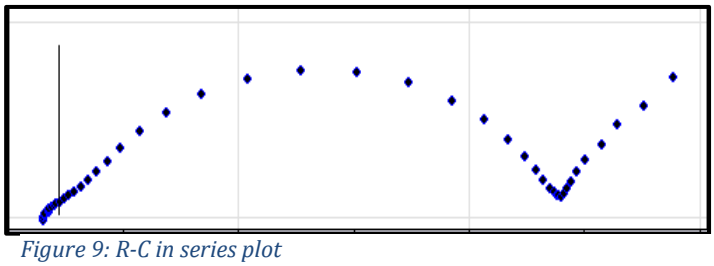

Figure 9: R-C in series plot

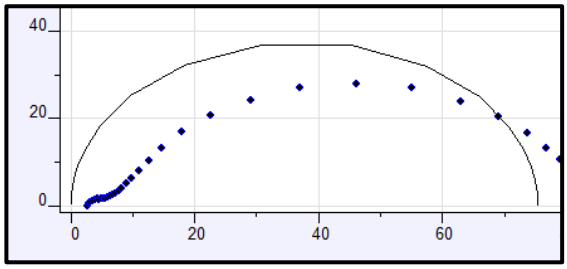

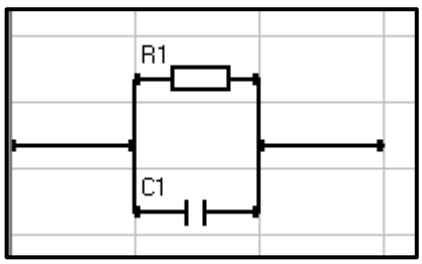

A particular type of capacitator is the constant phase element. When the battery's electrolyte is not liquid, an R-C parallel does not give the proper circuit. Because the double layer capacitance is not purely capacitive, therefor a constant phase element can be used if there is a solid electrolyte, in the figurer symbolized with a Q, with impedance eq. 13 and shown in Figure 12 [22, p. 179] In Figure 13 it can be seen how the semicircle have a more smooth form and do not start or end perpendicular on the x-axis, the α is a constant phase exponent, for a ideal capacitor it is 1, but else it is between zero and one

$$Z_{CPE} = \frac{1}{T(j\omega)^{\alpha}} \qquad Eq.13$$

Where ω is the Angular frequency, T is the parameter related to capacitance, Z_{CPE} is the constant phase impedance

Figure 11:R-C in parallel

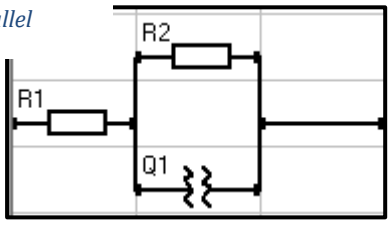

Figure 10: R-C in parallel

Figure 12: R + R-Q in parallel

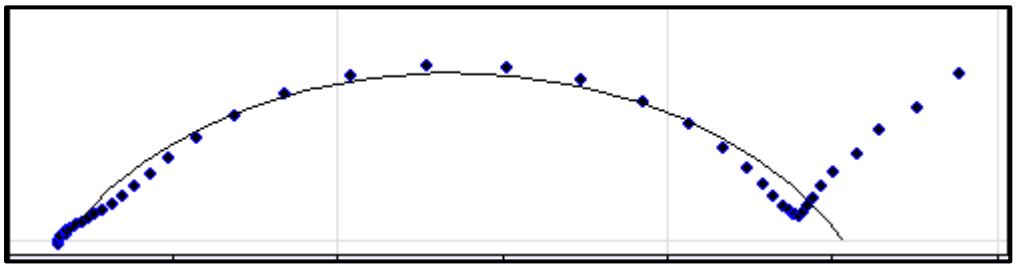

Figure 13:R + R-Q in parallel

A version of the constant phase element is a Warburg impedance, shown with a W in Figure 15 This is the impedance of mass transport, eq. 14 and the phase is set to a fixed value of 45 degrees that do not change with the frequency [22, pp. 90–95]. In Figure 14 the effect of the Warburg element can be seen as an approximately 45-degree plot in the right part of the figure.

$$Z_W = \sigma\omega^{-\frac{1}{2}} - j\sigma\omega^{-\frac{1}{2}} \qquad Eq.14$$

Where $\boldsymbol{\sigma}$ is the Warburg coefficient

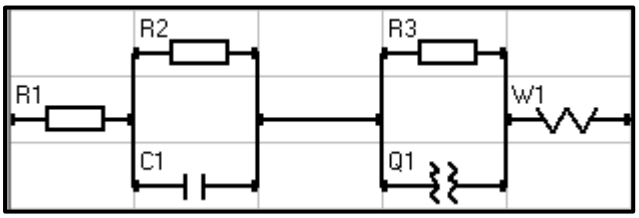

Figure 15: Equivalent circuit with Warburg

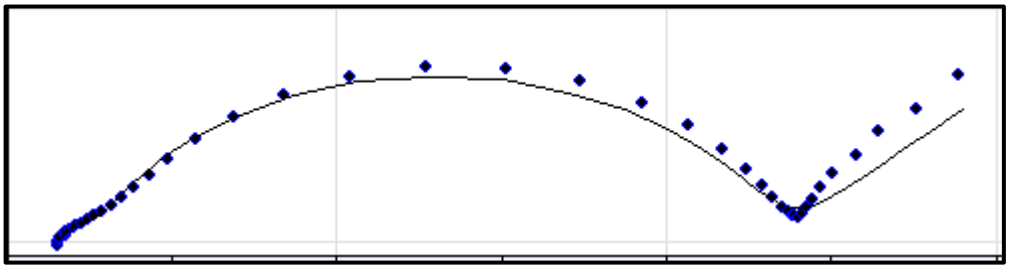

Figure 14: Equivalent circuit plot with Warburg

The inductor does also give imaginary reactive impedance, but its phase-shifting effect are opposite to the capacitator. Its values are so small that it is left out.

2.4.4 Nyquist plot analysis

Within a Nyquist plot of a battery cell, different regions can be found. An example can be seen in Figure 16. If the plot of the battery cell follows the real axis, it can be modelled by a simple resistor, as in case if the first region with R_b if the measurement also has imaginary components, it can be modelled by a combination of electrical components such as capacitors, inductances, and resistors as shown for the other regions. Figure 16 is used to help identify the equivalent circuit and its different regions in a lithium-ion battery cell.

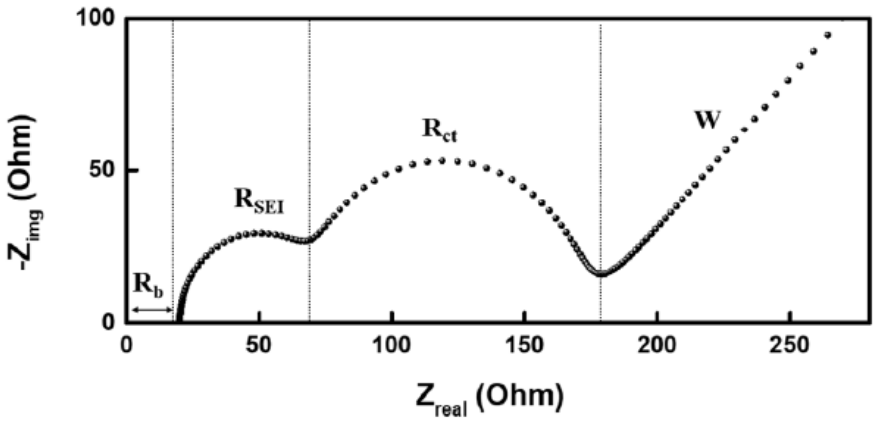

Figure 16: Lithium-ion battery electrochemical impedance spectroscopy plot with regions [21]

The first region R_b has only a real part, it marks the bulk resistance. This is the resistance of the different materials in the battery cell, like the current collector, separator, and electrolyte. The bulk resistance does not change much based on the SoC, but will change over time with many cycles, because of the different material change.

The second region R_{SEI} has both a real and an imaginary part. It can be modelled by a resistor and a capacitator C_{SEI}. It shows the interface layer between the electrode and electrolyte. This is created by a decomposition of the electrolyte.

The second semi-circle R_{ct} is the charge transfer resistance and double-layer capacitance $C_{electrod}$. This region is related to the electrochemical reaction, like the surface coating, particle size, bandgap structure and phase transition. Also, the temperature has a significant impact on the R_{ct}, and this is an important value to measure to get information on temperature dependence change in the battery.

In the last part, there is a straight line of 45 degrees. This is the mass transport region. To model this characteristic, a Warburg impedance W can be used. This impedance has a relation to the diffusion of lithium-ions. With a low concentration of electroactive species, the mass transport region and the charge transport will overlap. If there are a large concentration of redox species and a low current, the mass transport region almost disappear. [21]

2.4.5 Charge transfer

In the paper [*Electrochemical performance of modified artificial graphite as anode material for lithium-ion batteries - Wang et al. – 2013*][25], experiments with amorphous carbon-coated on synthetic graphite are done. Where there are used different amount of coating, in the impendence test there is used one type without coating and one with five weight per cent coting. The result on the impedance is shown in Figure 17; with the coting, there

is an apparent decrease in the real- axis impedance. There is resonated that this is because of an improved electrode reaction process.

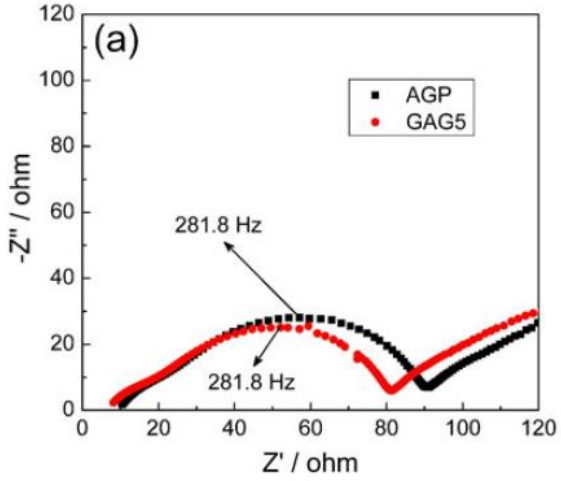

Figure 17 Difference in impedance with EIS [25]

There is also investigated the connection between charge transfer and coating in *Guo al et.*"[19] where the is seen a drop in charge transfer resistance that flown the amount of coating this can be seen in Figure 18 Charge transfer , where PVA0 is without coating and 0.4%,1%,1.4% and 2% for PVA5,PVA10,PVA15 and PVA20

Sample name	R_s (Ω)	R_f (Ω)	R_{ct} (kΩ)
PVA0	10.77	17.82	23.68
PVA5	10.67	15.26	6.437
PVA10	9.762	16.54	4.879
PVA15	7.725	16.05	3.529
PVA20	14.56	18.77	2.265

Figure 18 Charge transfer resistance

3. Research Questions

To measure the amount of carbon on a carbon material typical methods often used to characterise coatings are not possible to use, such as chemical analysis. Direct methods such as measuring the thickness in a microscope are also difficult to use due to the very thin coating layers. Nanometre range often requires the use of TEM (Transmission Electron Microscope), which is a time consuming and costly method. There is, therefore, a need to develop simpler and faster methods to quantify the amount of coating. Furthermore, the effect this has on the performance of the finished anode materials, such as resistivity. The aim of this work has therefore been to evaluate and develop methods with the use of TGA and EIS to characterise carbon coating on graphite. This leads to the following main research question:

- How can TGA be used to quantify the amount of carbon coating on graphite?
- How can EIS be used to quantify the effect of carbon coating on the performance of the anode material in a battery?

4. Methods

4.1 Limitation

There is some limitation for the test, first since this is a project in collaboration with the Elkem and it is an area they are researching, it is limited what information about the sample and the coating they will share to use in a published thesis. For this reason, the coating types and some other details are not used in the thesis.

Both the coated graphite samples and the battery cells is produced at Elkem and the experiments are limited to what and when they make it. This is a necessary arrangement since it is not facilitated produce at UiA, and it would be too complex for this thesis.

There are also some limitations on the equipment used at UiA. Both the TGA equipment and the EIS equipment are also used in other research. Especially the charging and discharging with the Iviumstat are problematic since this takes much time, and the access to the lab is limiting to regular work hours.

4.1.1 Equipment

To perform thermogravimetric analysis (TGA) and differential scanning calorimetry (DSC) analysis, UiA has two laboratory equipment from Mettler Toledo, TGA-1-HW and TGA-3-HT. They are controlled by a computer with specific software. Both equipment are partly automatic and can change crucible with pre-prepared samples and run it according to the program method. Both equipment can be divided into three integrated main parts, the sampling robot, the gas controller, and the oven. Each equipment also has a cooler, the cooler stand on the floor and are connected to the equipment for liquid cooling.

There is some difference between the equipment. The TGA 1-HW need a reference crucible inside the heating chamber of the same size as the one used for the sample. It is not necessary for the TGA-3-HT since it compensates for it through the software. The letters HT stand for high temperature. The TGA-3-HT can go up to 1600 Celsius while the TGA-1-HW only goes up to 1100 Celsius. While the TGA-3-HT can have a combined weight of the sample and crucible of one gram, in the TGA-1-HW, this weight can go up to five grams.

Figure 19 – From left: TGA-1-HW, separate weight used when distributing samples, kit to distribute samples and crucible.

4.1.2 Method

The method is the chosen program a sample goes through. It is composed of different stages that can be either dynamic or isotherm. Within the dynamic program, there is a heat change from the furnace, while within the isotherm program, the furnace holds a constant temperature. A method can contain many stages which come with several changes between dynamic and isothermal programs. It can also be a gas flow to each stage, so the stage of the test will be performed under a flow of the chosen type of gas. When a new method is made, a "blank" should be run before the method is used on a sample. This is a crucible of identical type as the one used for the sample that will go through the whole method to create a profile of the heat flux and changes caused by the crucible to later subtract from the test with a sample. When this is done, the "blank" profile gets saved with the method, and it is not necessary to perform again if there is no change in the method.
To determine the weight, the weight-in function is used. The crucible is here weighed by the machine without the sample in it and then weighed again with the sample before the test is started. This can be done with the same gas flow as in the first stage of the method. In all the tests, besides the two first ones. To avoid a big difference in the samples weight there is used a weight when the sample is distributed to the crucible to check the weight before it is inserted to the TGA equipment, shown in Figure 19

The analysation of TGA results can be done by using the built-in software. However, it is more practical to do it in excel and python. Only a pre-treatment consisting of normalising the data to its weight is done in the built-in software. To analyses the results and from the test Python is used.

4.1.3 Test materials

The different graphite samples are produced at Elkem Carbon, where the resistance was measured. At UiA, where the TGA test have been performed. There are two types of coating: coating type A and B. The samples are delivered and tested at different times. Therefore, also marked with a number right after the letter to show which group they are in. The last number after the hyphen is used to separate each sample. The reference samples are used as the base material for samples with the same type of coting. They are marked with "Ref" instead. Table 2 shows the information for each sample. Sample in group B4 are only used in the battery cell and are as graphite powder samples

Table 2 Sample types

Sample	Resistivity [μΩ*m]	Group
Type A1	Unknown	A1
Type A2-1	250.8	A2
Type A2-2	260.7	
Type A2-Ref	321.6	
Type B1-1	1176.4	B1
Type B1-2	1199.95	

Type B1-3	1054	
Type B1-4	841.1	
Type B2-1	1200	B2
Type B2-2	1160	
Type B2-3	674	
Type B3-Ref	1390	B3
Type B3-1	1050	
Type B3-2	704	
Type B3-3	441	
Type B3-4	750	
Type B3-5	547	
Type B3-6	668	
Type B3-Q	**-**	
Type B4-1	1083.7	B4
Type B4-2	Unknown	
Type B4-3	Unknown	
Type B4-4	1261.5	

4.1.4 Methods

There are six different program-based methods. The method is chosen partly on experience, consultation with the supervisors, literature reviews, and results of the earlier test performed. To show the methods clearly, they are written in tables with the parameters used. When describing the test, there will be referred to the method used. Moreover, if there are some changes, it will be explained in the test explanation.

Method one:

This method consisting of two stages and is shown in table [3]. This is the first method and is

Table 3 Method one

Start temperature (C°)	End temperature (C°)	Heat rate (C°/min)	Time (min)	Type	Gas	Gas flow (mL/min)
25	800	2.5	-	Dynamic	O2	50
800	800	-	60	Isotherm	O2	50

Method two:

The method, shown in table [4], is made to see the effect of using CO2 as gas.

Table 4 Method two

Start temperature (C°)	End temperature (C°)	Heat rate (C°/min)	Time (min)	Type	Gas	Gas flow (mL/min)
25	800	2.5	-	Dynamic	CO2	50
800	800	-	60	Isotherm	CO2	50

Method three:
The method, described in the table [5], consists of two stages. It is made to identify the effect of a more extended isotherm period and the use a higher temperature under CO2 gas.

Table 5 Method three

Start temperature (C°)	End temperature (C°)	Heat rate (C°/min)	Time (min)	Type	Gas	Gas flow (mL/min)
25	1000	2..5	-	Dynamic	CO2	50
1000	1000	-	300	Isotherm	CO2	50

Method four:
This method consists of four dynamic stages and four isothermal stages, cf. table [6]. N2 is used under the dynamic stages since no reactions shall occur. In contrast, O2 is used in the isothermal stages to investigate the reaction under a specific temperature.

Table 6 Method four

Start temperature (C°)	End Temperature (C°)	Heat rate (C°/min)	Time (min)	Type	Gas	Gas flow (mL/min)
25	640	2.5	-	Dynamic	N2	50
640	640	-	60	Isotherm	O2	50
640	660	2.5	-	Dynamic	N2	50
660	660	-	60	Isotherm	O2	50
660	680	2.5	-	Dynamic	N2	50
680	680	-	60	Isotherm	O2	50
680	700	2.5	-	Dynamic	N2	50
700	700	-	60	Isotherm	O2	50

Method five
This method consists of five dynamic stages and five isothermal stages, shown in table [7], where N2 is used under the dynamic stages since no reactions shall occur. In contrast, O2 is used in the isothermal stages to investigate the reaction under a specific temperature. A lower range of temperatures is used.

Table 7 Method five

Start temperature (C°)	End Temperature (C°)	Heat rate (C°/min)	Time (min)	Type	Gas	Gas flow (mL/min)
25	520	2.5	-	Dynamic	N2	50
520	520	-	60	Isotherm	O2	50
520	540	2.5	-	Dynamic	N2	50
540	540	-	60	Isotherm	O2	50
540	560	2.5	-	Dynamic	N2	50
560	560	-	60	Isotherm	O2	50
560	580	2.5	-	Dynamic	N2	50
580	580	-	60	Isotherm	O2	50
580	600	2.5	-	Dynamic	N2	50
600	600	-	60	Isotherm	O2	50

Method six

This method consists of three dynamic stages and three isothermal stages, shown in table [8], where N2 is used under the dynamic stage since no reactions shall occur. In contrast, O2 is used in the isothermal stage to investigate the reaction under a specific temperature. A lower range of temperatures used than in method five and a higher difference in step temperature.

Table 8 Method six

Start temperature (C°)	End Temperature (C°)	Heat rate (C°/min)	Time (min)	Type	Gas	Gas flow (mL/min)
25	440	2.5	-	Dynamic	N2	50
440	440	-	60	Isotherm	O2	50
440	480	2.5	-	Dynamic	N2	50
480	480	-	60	Isotherm	O2	50
480	520	2.5	-	Dynamic	N2	50
520	520	-	60	Isotherm	O2	50

4.2 Performed TGA Tests

There are used aluminium oxide crucible for all the tests. They are available in two different sizes, 150 [uL] and 70 [uL]. The used crucible size is specified for each test.
The tests are categorised into four different chapters, after which type of test it was. Under each chapter, the test is in chronological order and named by the number to separate them and the coating type.

4.2.1 Flow test

A flow test is performed, where three different flow rates of oxygens are used to investigate the effect of the gas flow. The different flow parameters are chosen based on earlier experiments and consultations with the lab engineer and supervisors from Elkem. It is essential that the gas flow does not blow away the sample powder and still give enough oxygen for a reaction to happen. The sample also has a large amount of Type A1 coting, and it can therefore indicate which temperature area is of interest. For this test, one is used, with a change in the flow rate and parameter shown in the table [9].

Table 9 Flow test

Sample	Weight [mg]	Position	Flow [mL/min]	Crucible [uL]
A1	16.8952	111	30	150
A1	13.3687	112	50	150
A1	18.7573	113	60	150

4.2.2 Oxygen tests

There are seven tests with oxygen on four different samples groups, where some groups are tested more than once. Oxygen test one, cf. table [10], is done with method one. The sample is not weighted when distributed. That can give a difference in sample size. Oxygen test two, cf. table [11], is also done with method one. Within this test, a different weight is used when the sample is distributed. In oxygen test three, shown in table [12], method one is used, and all samples without the quartz sample are measured while distributed. The quartz sample is a solid piece. For oxygen test four, shown in table [13], method one is used. This is a re-test of oxygen test two and is done three times, where

the last time 10 [mg] are used. Here are the samples that are measured with a different weight when distributed. Oxygen test five, shown in Table 14 is done two times. Here, method one is applied.

Table 10 Oxygen test one coating type B1

Sample	Weight [mg]	Position	Crucible [uL]
Type B1-1	32.9930	110	150
Type B1-2	23.8954	111	150
Type B1-3	27.7753	112	150
Type B1-4	28.5663	113	150

Table 11 Oxygen test two coating type B2

Sample	Weight [mg]	Position	Crucible [uL]
Type B2-1	24.3362	102	150
Type B2-2	23.1533	103	150
Type B2-3	25.4446	104	150

Table 12 Oxygen test three coating type B3

Sample	Weight [mg]	Position	Crucible [uL]
Type B3-Q	31.8332	106	150
Type B3-Ref	27.7039	107	150
Type B3-1	24.8582	108	150
Type B3-2	26.6851	109	150
Type B3-3	25.1834	106	150
Type B3-4	26.6888	107	150
Type B3-5	26.4263	108	150
Type B3-6	28.1059	109	150

Table 13 Oxygen test four coating type B3

Sample	Weight [mg]	Position	Crucible [uL]
Type B2-1	24.2019	106	150
Type B2-2	24.6939	107	150
Type B2-3	23.2156	108	150
Sample	Weight [mg]	Position	Crucible [uL]
Type B2-1	23.8698	107	150
Type B2-2	25.2745	108	150
Type B2-3	24.4682	109	150
Sample	Weight [mg]	Position	Crucible [uL]
Type B2-1	8.9817	106	150
Type B2-2	10.6172	107	150
Type B2-3	10.8627	108	150

Table 14 Oxygen test five coating type A2

Sample	Weight [mg]	Position	Crucible [uL]
Type A2-1	24.4733	106	150
Type A2-2	24.6190	107	150
Type A2-Ref	24.3421	108	150
Sample	Weight [mg]	Position	Crucible [uL]
Type A2-1	21.4554	106	150
Type A2-2	25.6130	107	150
Type A2-Ref	22.6852	108	150

4.2.3 Carbon dioxide tests

There are two tests with CO2. The first test is shown in the table [15]. Here is method two used. TGA 3 is used since it already had CO2 connected. The samples are weighted when distributed. In the second CO2 test, shown in table [16], method three is used, and smaller samples are used. They are weighted when distributed.

Table 15 CO2 test coating type B1

Sample	Weight [mg]	Position	Crucible [uL]
B1-1	32.9290	110	70
B1-2	23.8416	111	70
B1-3	27.7082	112	70
B1-4	28.1007	113	70

Table 16 CO2 Hight temperature

Sample	Weight [mg]	Position	Crucible [uL]
B1-3	13.3824	110	70
A1	12.2006	111	70

4.2.4 Step tests

There are three step tests done with the same samples but different methods. In step test one, shown in table [17], method four is used. It is performed only on four out of the six planned samples because the machine was inaccessible for a week. The test is done with TGA 1 since this had both O2 and N2 connected. Step test two is done with method five and include six samples shown in table [18]. TGA 1 is also used for this test. Step test three is performed with method six and is shown in table [19]. It is performed with TGA 1. In all the step test, the samples are weight when distributed.

Table 17 Step six hundred degrees

Sample	Weight [mg]	Position	Crucible [uL]
B3-Ref	26.0073	107	150
B3-3	23.5572	108	150
B3-4	25.5003	109	150

A2-1	23.8967	110	150

Table 18 Step five hundred degrees

Sample	Weight [mg]	Position	Crucible [uL]
B3-Ref	25.8016	102	150
B3-3	26.5621	103	150
B3-4	26.5508	104	150
A2-1	26.4541	105	150
A2-2	25.6724	106	150
A2-Ref	26.2348	107	150

Table 19 Step four hundred degrees

Sample	Weight [mg]	Position	Crucible [uL]
B3-Ref	23.1750	103	150
B3-3	24.6826	104	150
B3-4	25.4798	105	150
A2-1	24.9072	106	150
A2-2	26.6118	107	150
A2-Ref	23.9262	108	150

4.3 Electrochemical impedance spectroscopy

4.3.1 Equipment

To do the EIS tests, an IviumStat.XRi, hereafter only referred to as Iviumstat, is used. This is an instrument from Ivium technologies that can be used for multiples purpose, here used for EIS measurements as well as charging and discharging of batteries. It is a very sensitive instrument. The used the cable that follows the instrument is shown in **Error! Reference source not found.**. A test cell called “TestCell1” has two cables “GND” (green) and “WE2” (red) connected to it. There are different ways to connect the cables to the battery or other specimens. In this work a two-terminal sensing and a Four-terminal sensing are used, With the two-terminal connection, “WE” (red) and “S” (white) are connected together as well as “CE” (black) and “RE” (blue) are connected together. Then each set of cables are connected to the electrode and the counter electrode. With a Four-terminal connection, “WE” and “CE” is connected to the different electrodes and “S” and “RE” is separately connected as sensors and reference. The connection to the battery holder can be seen in **Error! Reference source not found.**.

There is also a coin cell battery holder from Ivium technologies, which can be seen in Figure 20. There is an extra cable between the cables from the Iviumstat and the holder. This is because there is a misfit, and the cable is somewhat loose without this. There is a signal without, but especially when a battery is shifted, it is hard not to touch the cable, and some irregularities in the measurement can be seen. To be sure the loose fit does not affect the measurement. The extra cables er cut on the measurement of set two and three, and only the end is used.

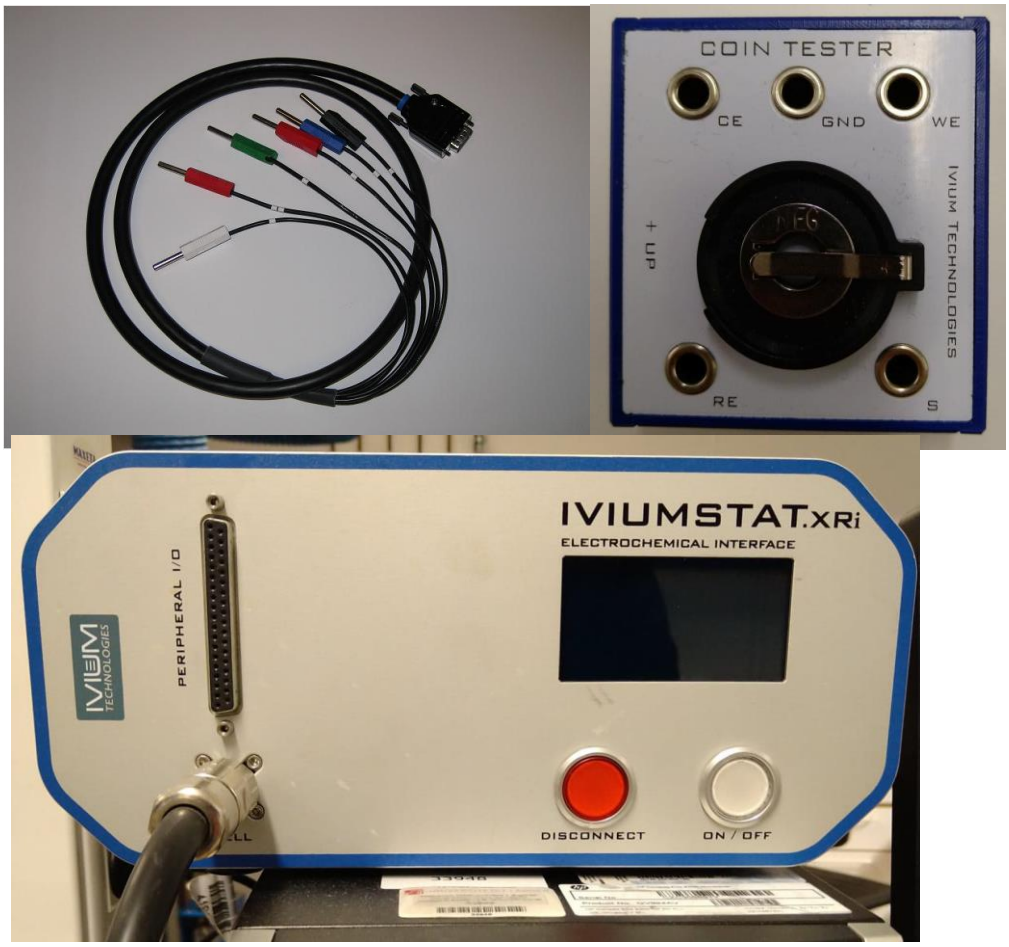

Figure 20 Top left: Iviumstat cables. Top right: battery holder from Ivium. Bottom: Iviumstat

4.3.2 Measurement parameters

Different values can be found for the ESI measurement. For this test, there is a focus on the charge transfer resistance. There are two different charge transfer values in the measurement, one for the cathode and one for the anode. These values are sometimes possible to separate as two semicircles, but often they merge into one. Therefore, it is better to look at the total value of both charge transfer resistances. The cathode part of the batteries is the same in all the cells, so it will still show the difference between the cells and can be used to find a pattern. The Warburg impedance can also be seen, but it is not used, and therefore the measurement is not customised to cover this frequency range. The parameters used are mainly obtained by trial and error and consultation with the supervisors. It is also confirmed by other related research, like “Characterisation of batteries by electrochemical impedance spectroscopy» [13].

The internal resistance can also be seen, but it changes based on which voltage is used and the amplitude voltage. The SEI layer resistance can be seen on some test, but it is hard to define precisely. It is a small value compared to the charge transfer.

On set one and set two with batteries, all tests done with two different amplitude. The amplitudes and the other parameters can be seen in Table 20; the parameters for set three are given in Table 21. For set three, only a test with one amplitude is done.

Table 20 EIS measurement parameters Type A2 and B4.

Measure-ment	Control	Frequency max [Hz]	Frequency min	Amplitude voltage [V]	Current range [mA]	Frequency each decade	Frequency in total
One	Voltage	1000000	0.05	0.01	10	6	45
Two	Voltage	1000000	0.05	0.1	10	6	45

Table 21 EIS Measurement parameters PAT-cells.

Measure-ment	Control	Frequency max [Hz]	Frequency min	Amplitude voltage [V]	Current range [mA]	Frequency each decade	Frequency in total
One	Voltage	1000000	0.01	0.01	10	6	49

It is also necessary to choose a potential for "E start "for each measurement. This need to be changed for each battery to follow the potential in the batteries. On the 0.01 V amplitude measurement, the exact battery potential is used, since the amplitude changes the potential only by 0.0001 V. when the 0.1 V amplitude is used, it is used also sets the batteries exact values. The parameter window can be seen in Figure 21

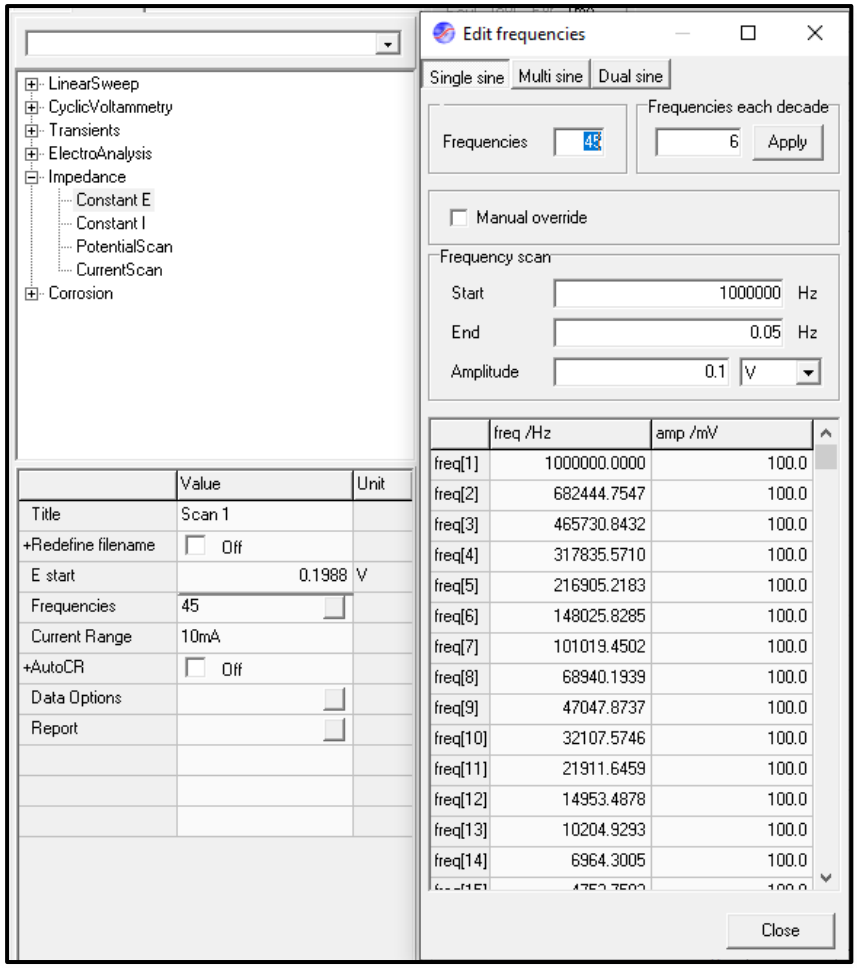

Figure 21 EIS parameters window

4.3.3 Batteries

Two types of cells are used, first button-cells, this is later changed to pat-cells because of some difficulties with the production of the cells at Elkem. The number of each type of cell and their coting is given in Table 22 Batteries cells

Table 22 Batteries cells

Cell type	Coting	Number of cells	sets	Date charge
button-cell	**Type B4-1**	3	1	01.252021
button-cell	**Type B4-2**	1		
button-cell	**Type B4-3**	3		
button-cell	**Type B4-4**	2		
button-cell	**Type A2-Ref**	2	2	24.03.2021
button-cell	**Type A2-1**	2		
Pat-cell	**Type B3-Ref**	1	3	
Pat-cell	**Type B3-Ref**	1		
Pat-cell	**Type B3-3**	1		

The cells are produced at ELKEM and are tested there before they are delivered to UiA. Due to this timespan an SEI-layer is produced and the cells loses some of their capacity. They were delivered with an SoC close to zero and a potential around 1 [V] in set-one. The second set was instead delivered with an SoC of 80 % and potential between 0.08 V and 0.09 V. The third set was delivered with an SoC of 92 %, then taken back and charged down to 80 %

4.3.5 Tests

There is done tests on three different coating types of batteries. The test is explained in each sub-chapter. It is given an overview in Table 23 where the EIS test is done at the SoC levels marked with "x"

Table 23 Overview of SoC % with EIS

Cell Type	OCV	92 % SoC	80 % SoC	50 % SoC	20 % SoC
Type A2	-	-	x	x	x
Type B1	-	x	x	-	-
Type B4	x	-	x	x	x

Test of Type B1-1 to B1-4

B4-1 to B4-4 is the first to be tested. Here one battery with each material type in the set is used. The batteries have first been delivered with an approximately 0% SoC. There is an EIS measurement done with each cell with the parameter listed in table [20]. After this, all batteries in the set, without one that was charged with the Iviumstat at UiA, are delivered to Elkem, and they charge them to 100 % SoC. They are then deliver back to UiA and an EIS scan on the same batteries is then done with the parameters shown in table [20]. The low amplitude is always done first since the high one can make some potential change in the battery. After this, the batteries are discharged to 80% SoC with the Iviumstat. There is a new EIS performed at 80%. The following discharge is also done with the Iviumstat and EIS is performed at each SoC level. To perform the discharge to SoC 80 %, 50 % and 20 %, there is calculated SoC % form the charging data from Elkem. There is also a calculated a potential to each SoC level, and this values are used to fin the parameter for the discharge with the CCCV method.

The charging equipment at Elkem log alle relevant information about the process. This includes for each time step, potential, current, and time. There are also some cumulative values logged such as capacity and energy. With these value the SoC is calculate based on Eq. 15 for each time step. The potential level is also calculated with Eq. 16. This was done for all the time steps. Subsequently, the values with the chosen SoC were extracted and used to calculate the discharge rate and time, with Eq. 17 and Eq. 18.

$$SoC = \frac{Culumuiavti\ capacity}{Totale\ capacity} \qquad \frac{mAh}{mAh} \qquad \text{Eq15}$$

$$V = \frac{Energy}{Culumuiavti\ capacity} \qquad \frac{mWh}{mAh} \qquad \text{Eq.16}$$

$$Discharge\ current\ = \frac{Average\ capacity * active\ mass}{1000} * C \qquad \frac{mAh * mg}{1000} C \qquad \text{Eq.17}$$

It is divided by 1000 since the average capacity is given in mAh/g

$$Discharge\ time(s) = \frac{\Delta Capacity}{Discharge\ current} 3600 \qquad \frac{mAh}{mA} * 3600 \qquad \text{Eq.18}$$

The delta capacity is the charged capacity between each level of SoC used.

Test of Type A2-1 and A2-Ref

Since the result of the discharge process had some error and it is hard to get the right potential in the CV part of the discharge. It was chosen to start at 80 % SoC from Elkem. And only use CC-discharge to 50 % SoC and 20% SoC. To achieve stability in the cells, a C-rate of 1/20 was chosen for the discharge instead of 1/10 C-rate. The calculation was done with charging data from Elkem. The discharge for the first to cells A2-1- 1 and A2-Ref-1 was done with the Iviumstat. There was an EIS measurement done at each SoC level. The A2-1-2 ang A2-Ref-2 batteries were instead discharged with a NEWARE battery testing system at UiA. The calculation was done the same way with the use of Eq. 15,16,17 and 18. Since there only was a CC part in the discharging, the voltage calculation was only used to compare the potential with the calculated values after discharging.

Test of PAT-cells

The PAT-cell was used since there were some problems with making button-cells. There is no appropriate equipment to do the charge or discharge at UiA. Thus, it was necessary to test the cells at Elkem and then bring them back to discharge at UiA. Therefore, only two different SoC levels have been investigated by EIS measurements. The used parameters for the EIS are shown in Table 21. The PAT-cell makes it possible to do some different measurements since it is constructed with a reference between the two sides of the cell. And It is possible to measure only one side of the cell, either the cathode or the anode side.

Analysing of the EIS data

To analyse the EIS measurements, the Ivium software was used. Within that, there are possibilities to make an equivalent circuit with the elements mentioned in the theory chapter. The software then makes a model of this. To find the best fitting parameters for the model, it uses the minimum sum of the square. The formula is given in Eq. 19, where n is the number of data points, $f(x)$ is the equality model. After this, the error for the parameter is calculated with the formula Eq. 20 where i is the parameter and p_i is the parameter value, and C_{ii} is the diagonal entry of the estimated covariance matrix C The error for the R_{ct} is tried to be kept as low as possible. Since there is only the charge transfer resistance investigated in the thesis, it would be possible to only focus on this parameter/measured plots.

$$Minimum\ error = \sum_{i=1}^{n} f_1(x)^2 \qquad \text{Eq.19}$$

$$Error_i = \frac{100 C_{ii}}{p_i} \qquad \text{Eq.20}$$

Errors

In the first set of batteries, the calculated SoC did not seem to match the real one perfectly. The CV part of the discharge did not reduce the charge of amp to an acceptable level quickly. Therefore, it was standing on a higher value, between 0.050 mA and 0.2 mA and kept on discharge instead of stabilising. If it was aborted, the potential in the cell was measured with a difference from the calculated one. It was not the same in all cells, and it was always within the nearest 10 % from the calculated one. The error was more significant at low SoC %. It can still make a significant difference in the charge transfer measurement, especially at low SoC %. It is not clear what causes it, but the cells were not completely full when started, resulting in a calculation error. At the same SoC there will also be a difference in the potential, based on a discharge or a charge. It is not sure the calculation of potential will be correct.

An error was also discovered in the internal resistance part of the measurement. This was because of some bad connection between the cables and the battery holder. The error was fixed using some extra plugs in between the battery holder and the cables and the tests where repeated.

A Error when performing the EIS happen multiple times. Instead of going on to a the next frequency, the same frequency was repeated several times and this increased the potential in the cell by up to 10 %, it did usually fall to 1-2% after some time. It still made some difference in later measurements. A plot of how a typical error in the measurement look, can be seen in Figure 22.

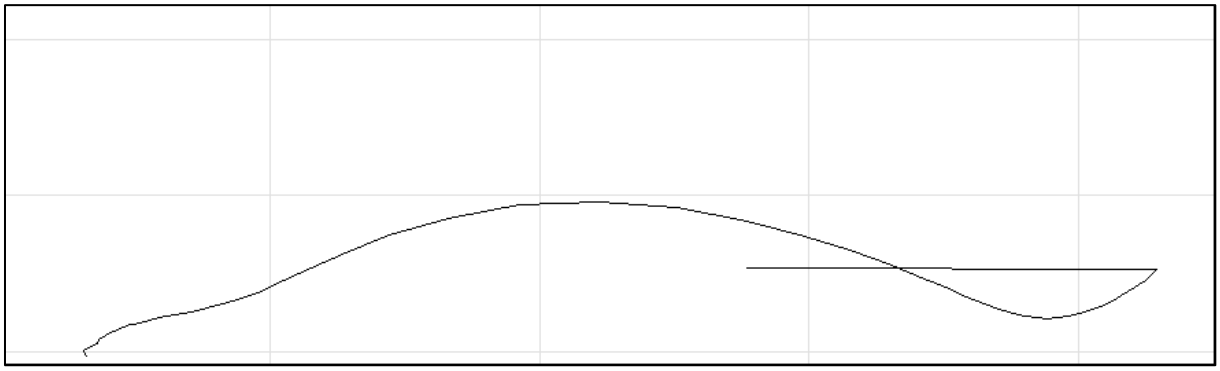

Figure 22 EIS error

4.4 Plotting and analysing

There is used python to calculate and plot the results. For the EIS analyses the Ivium software is used. Only the reference temperature is used for the results.

4.4.1 Linear regression

To make the regression graph a function in python is used, the make a simple linear regression. A genera equation for the line is given in Eq. 21

$$Y_i = a + b * x_i + e_i \quad \text{Eq.21}$$

Where e is an error

4.4.2 Interpolation

There is interpolated when the weight loss is used at an exact temperature to get exact numbers when plotting. This does not have much affection on the number, but it makes it more standardised to work with. A TGA test consists of between 22000 and 44000 measuring points. The interpolation is one in python, the general equation for interpolation is shown in Eq. 22

$$y = y_1 + (x - x_1) * \frac{y_2 - y_1}{x_2 - x_1} \quad \text{Eq.22}$$

4.4.3 Start noises

There is some noise in the measurement at the start. Hence, the different samples start at some difference in weight per cent, with such small changes that are looked at here, it will influence the result. All the values from the TGA measurements are therefore divided on their own weight per cent at 50-degree Celsius and multiplied by 100 to remove the starting error.

5 Results

5.1 TGA

5.1.1 Flow test

To investigate the effect of the flow rate and indicate the weight profile of coated graphite oxidation when heated. A sample with coating Type A1 is used. It is heated with a rate at 2.5 C/min and under three different flow rate with oxygen, 30 mL/min, 50 mL/min and 60 mL/min Figure 23A and Figure 23B shows the same graph, but the x-axis changes in Figure 23B to see how the different flows affect the weight loss rate. In Figure 23A, a weight loss of 2.5 % around 580 degrees can be seen, while the rest of the graphite sample is burned completely between 700 and 800 degrees Celsius. The peaks can be seen both when plotting the derivate of the weight change Figure 23D and the heat flux Figure 23C. The heat flux shows a clear exothermal peak at the temperature of highest oxidation rate (burning) of the graphite at around 750 degrees Celsius, but also a small peak can be seen at around 580 degrees Celsius. the increased flow rate gives a higher oxidation rate. Based on the experiment, a flow rate of 50 mL/min was chosen as a standard for the rest of the experiments, to give å adequate oxidation for complete burning of the sample, but still limiting the oxidation rat enough to observe the difference between the materials easily

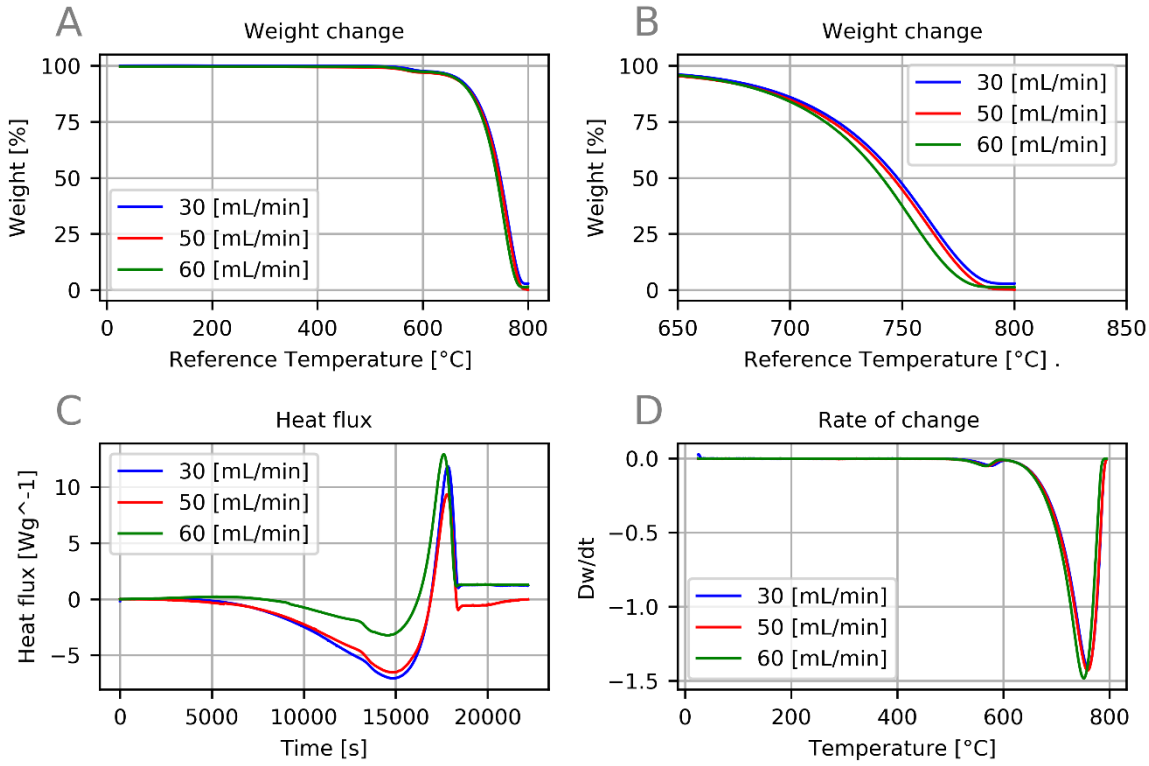

Figure 23 Flow test; A) shows the whole temperature range. B) shows the main reaction area. C) shows the heat flux at different time. D) shows the rate of change in weight dividend on the change in temperature

5.1.2 Oxygen tests

Test of Type A2 coating

The test with Type A2 coated samples in oxygen shows a weight loss at different temperature of the samples. In Figure 24A, there is a clear difference between where the

main weight loss happens. By zooming in on the y-axis, there can also be a difference in weight loss at an early stage in Figure 24B. The heat flux in Figure 24C also shows a difference in the three samples. In this graph the weight at 50 degrees Celsius is set to 100 % weight. The second test of the same samples was done to see if the results were the same, shown in Figure 25 There is not a big difference, but there can be seen that A2-Ref are a little lower before the weight drop. There is also used a simple linear regression at each test. This is done to see in which degree the temperature at 50 % weight loss happen has a correlation to the resistivity. Figure 26

To find the weight loss of sample A1, it is plotted in the same graph as the A2 samples in Figure 24 And the difference between the reference samples A2-Ref and samples A1 is calculated at the different temperatures where it is possible to see the first oxidation process weight loss rate flattens. There is 585 degrees Celsius when it starts to flatten, 600 degrees Celsius in the middle and 625 degrees Celsius right before it starts to fall with a higher rate again. This can be seen in Table 25 Where the weight loss is around 2.5%. The A1 sample is assumed to have a much more significant amount of coating than the rest. And it can be seen that the others do not have this separation between the first and second oxidation process.

In the Table 26 the weight difference from the reference sample A2-Ref is calculated at three different temperature to be able to compare it with the step test method

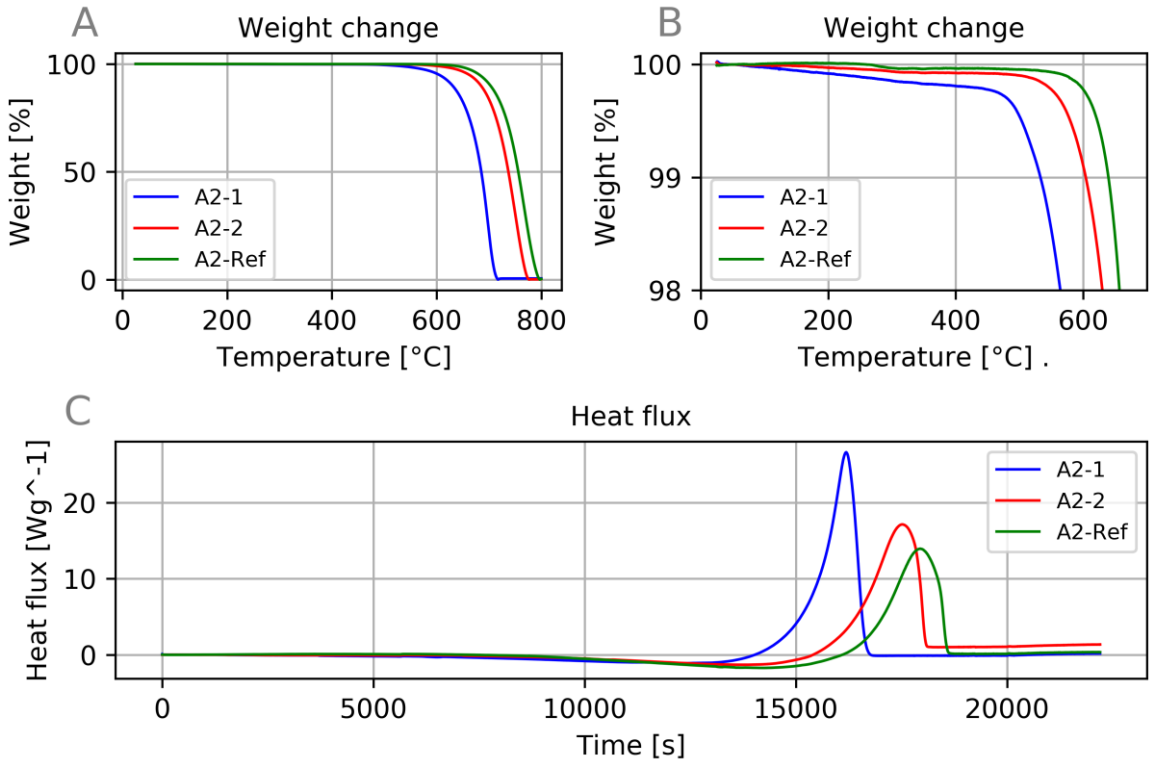

Figure 24 A shows the weight change related to the temperature. B is zoomed in on the first 2 % weight change. C shows the heat flux related to the time.

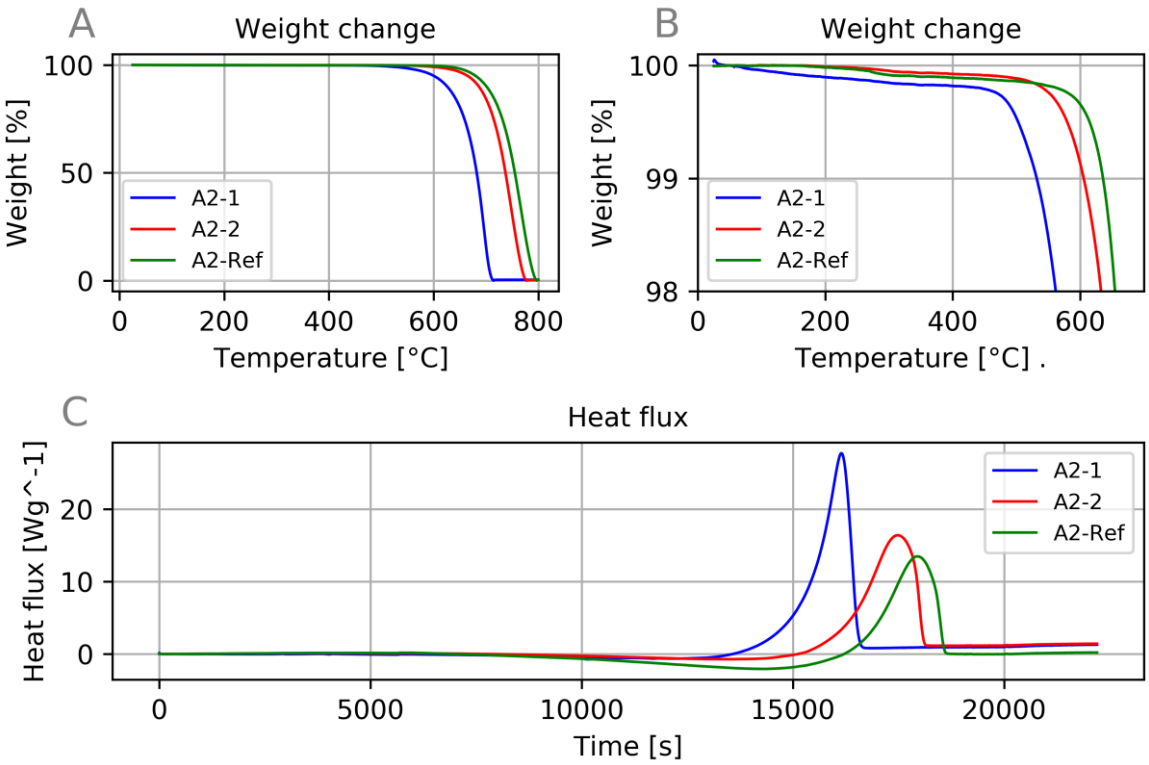

Figure 25 A shows the weight change related to the temperature. B is zoomed in on the first 2 % weight change. C shows the heat flux related to the time.

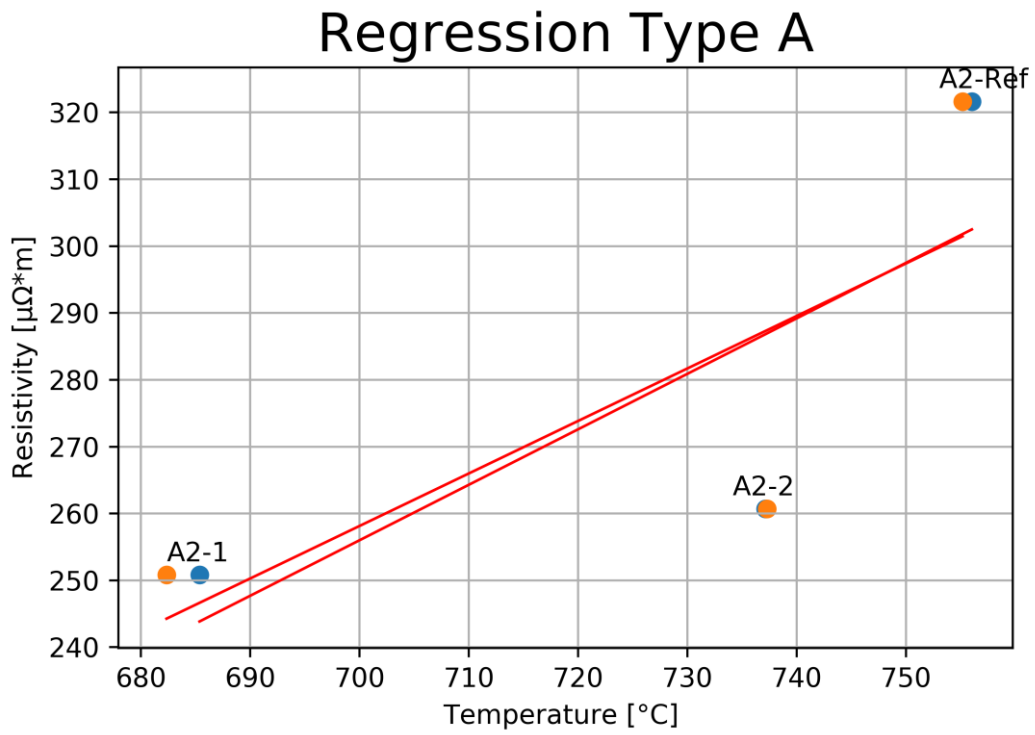

Figure 26 Regression plot of Type A at 50 % wt.

Table 24 Comparing of A2 Types coating and A1 Type coating

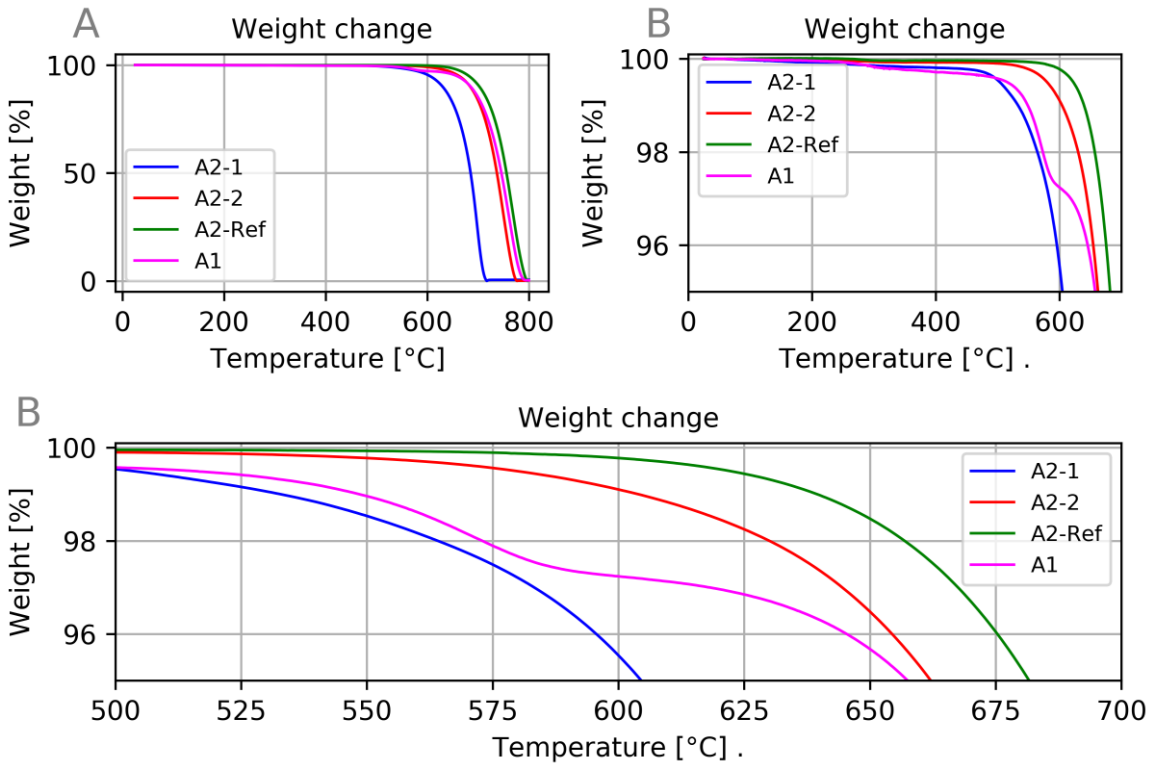

Table 25 weight difference Type A1 and A2-Ref

	A1	A2-Ref	Delta
Weight 585 °C	97.487 %	99.858 %	2.370 %
Weight 600 °C	97.238 %	99.778 %	2.540 %
Weight 625 °C	96.849 %	99.440 %	2.591 %

Table 26 Weight difference of all Type A

	500 °C		550 °C		580 °C	
Sample	Weight	weight difference	Weight	weight difference	Weight	weight difference
A2-1	99.542	0.414	98.535	1.398	97.208	2.669
A2-2	99.903	0.053	99.778	0.154	99.495	0.381
A2-Ref	99.956	0.000	99.932	0.000	99.876	0.000
A1	99.577	0.379	98.960	0.972	97.667	2.209

Test of Type B1 coating

The test of coating Type B1 shown in Figure 27 also gives some difference between the temperature where the weight fall happens and the different samples. This can also be seen at the heat flux graph, and no drop in weight before can be seen. To show the

difference clearer, there is plotted a linear regression of the temperature when the weight crosses 50 % wt. and the material resistivity. This is shown in Figure 28 coefficient of determination: 0.968

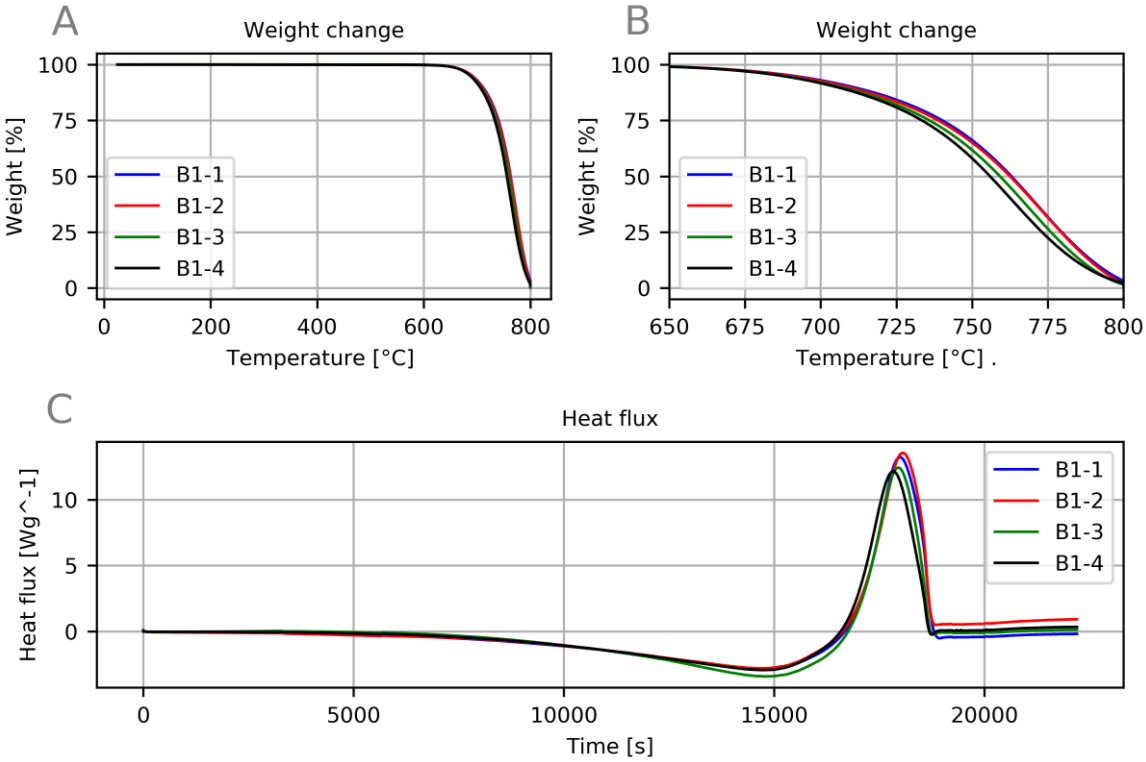

Figure 27 Test of Type B1 coating in O2; A shoes the whole temperature range. B is zoomed in on the weight fall. C shows the heat flux.

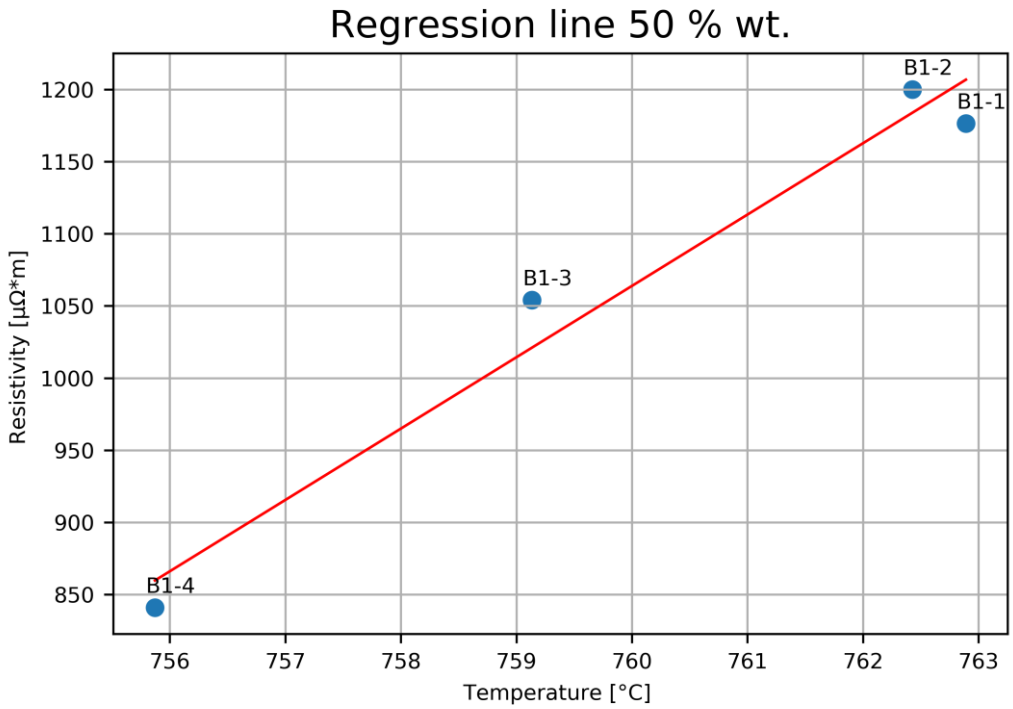

Figure 28 Regression line of coating Type B1

Test of quartz sample

The quartz sample is coated with a B3-Q, there is possible to detect a weight loss between 550-degree Celsius and 575-degree Celsius, seen in [A]. This can also be seen in [B], the heat flux jumps with a peak just above 550 degrees Celsius. In [C], the rate of rate of change is shown [D]

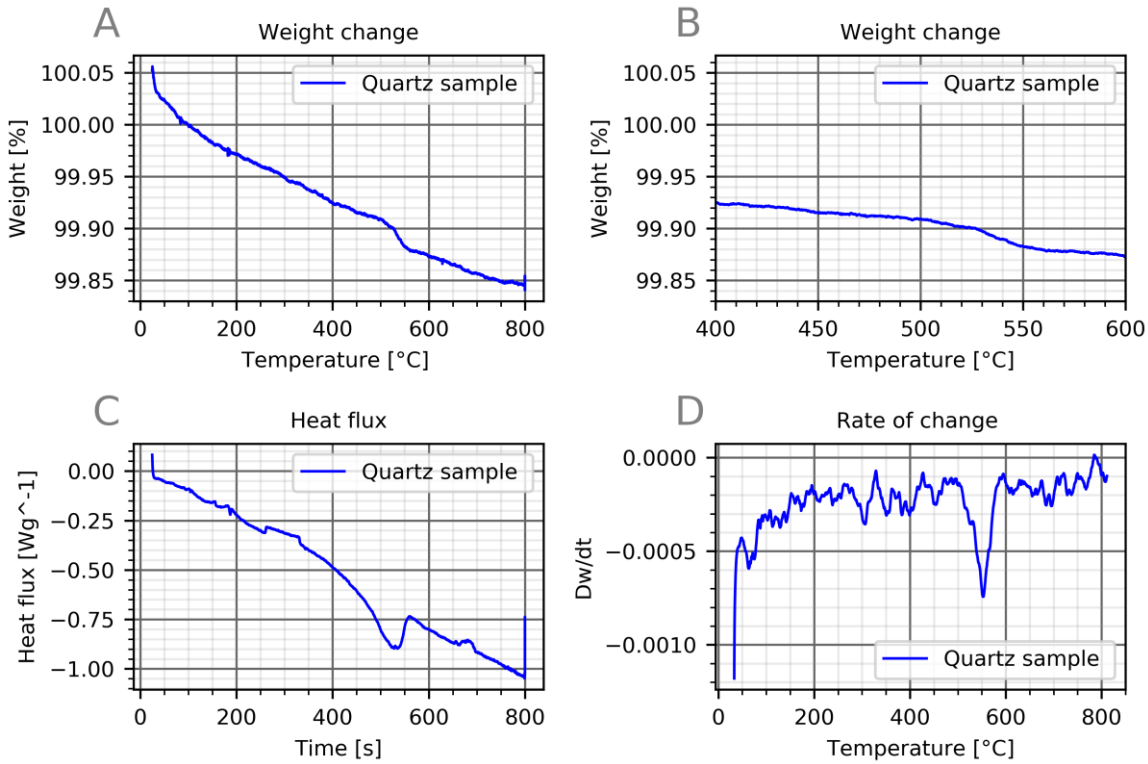

Figure 29 ; A shows the weight change in the whole temperature range. B Shows clearer the drop in weight. C Shows the heat flux. D Shows the rate of change

Test of coating Type B3

There is no clear connection between the weight loss for the samples on oxygen type B3 coating and a large portion of the weight loss like in coating Type B1, It is therefore focused on an area, where the weight has dropped to 99.6 %, where the coating can have be oxidating but not as much of the base material, this is the point where the B3-3 go from a slow fall rat to a rapid one, where they may by more graphite that is oxidizing. To isolate the effect from the coating. The regression can be seen in Figure 31

There is also extracted the weight at 500 degrees Celsius and 580 degree Celsius and calculate the difference from the reference sample B3-Ref, shown in Table 27. On 500 degrees Celsius has of the sample has a negative weight difference from the reference. This indicates that it is not a good temperature or method to measure the coatings weight. On 580C, only sample B3-1 has a negative difference from the reference. This is also the sample with the highest resistivity. This looks like a better temperature to use.

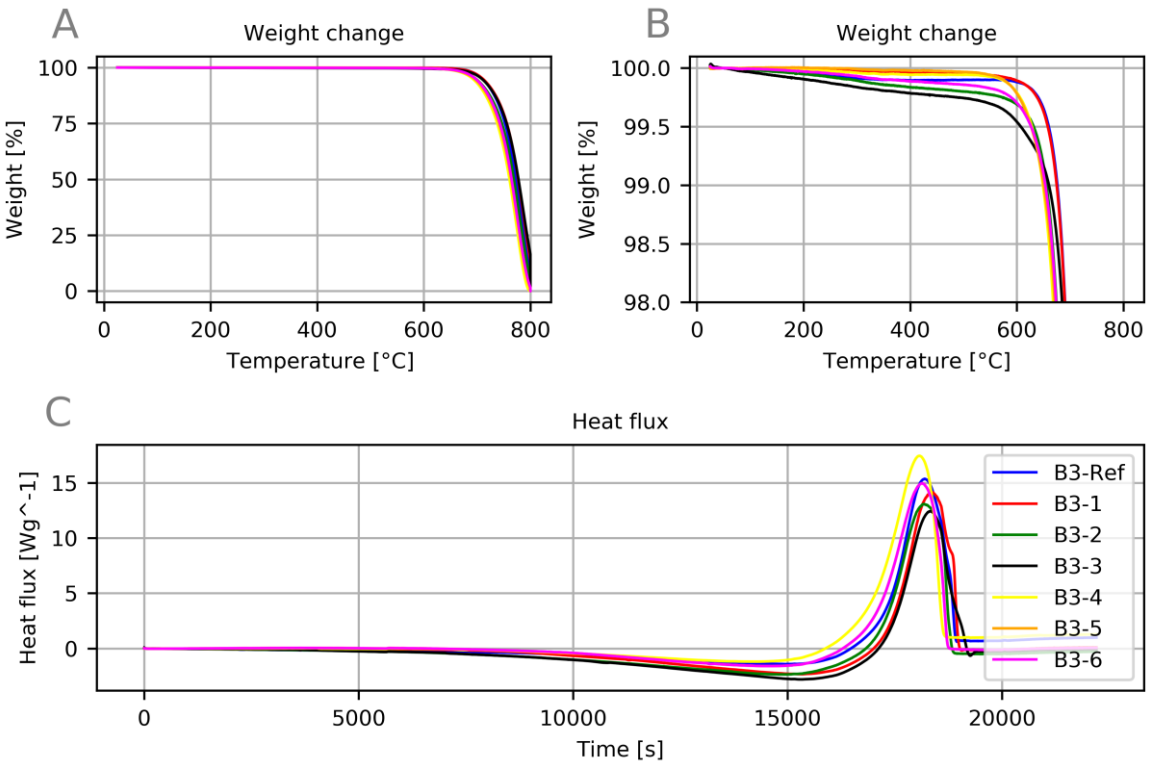

Figure 30 Type B3 coating; A shows the weight change. B shows the first 2 % weight change. C shows the heat flux.

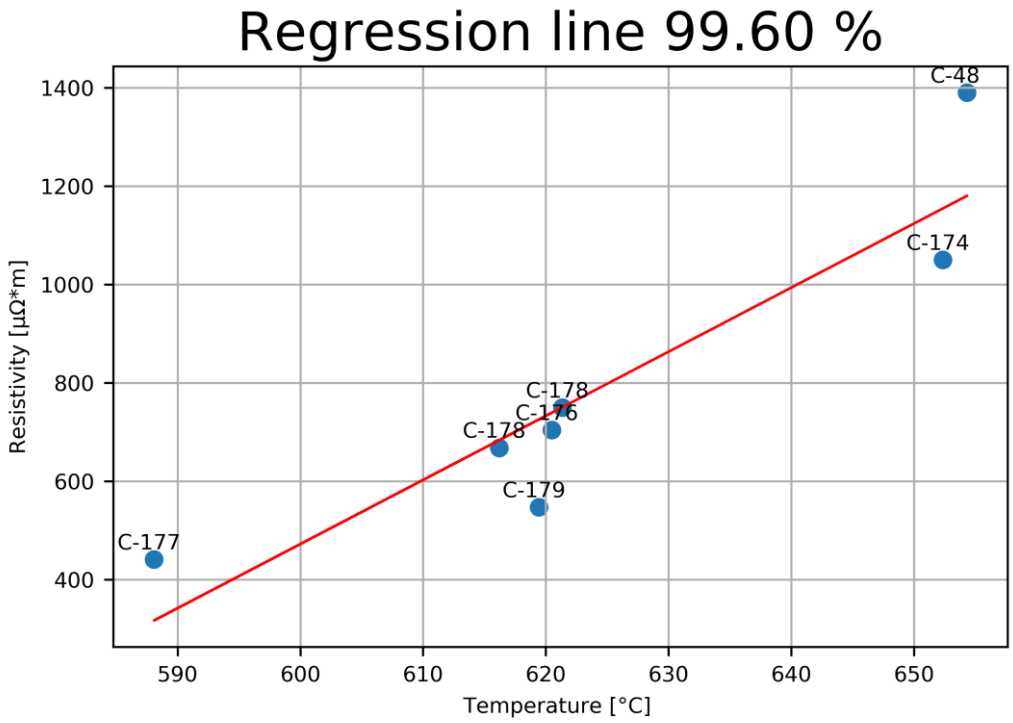

Figure 31 Regression of Type B3 coating at 99.6 %

Table 27 Weight loss at 500 degrees and 580 degrees

	580 Degree Celsius		500 Degree Celsius	
Coating	Weight	Weight loss relative to reference	Weight	Weight loss relative to reference
B3-Ref	99.895		99.899	0
B3-1	99.918	-0.0240	99.955	-0.0555
B3-2	99.738	0.1575	99.8	0.0992
B3-3	99.630	0.2654	99.744	0.1548
B3-4	99.880	0.0149	99.943	-0.0435
B3-5	99.884	0.0116	99.967	-0.0677
B3-6	99.778	0.1170	99.858	0.0415

5.1.3 Carbon dioxide tests of Type A1 and B1

The CO2 test of B1-1 to B1-4 did not give any apparent weight loss when run up to 800 degrees Celsius and stayed isotherm there for an hour in carbon dioxide of Type B1, shown in Figure 33. For sample A1 and B1-3 that when tested up to 1000 degrees Celsius and staying isotherm there for 5 hours, in CO2, shown in Figure 32. There was a weight loss, here the Type A coated sample A1 lost around 15 % weight. The Type B1-3 coated sample lost around 50 %, but since each test takes more than 10 hours, and there was no sign that a separate weight loss for the coating was happening, it was not tested further.

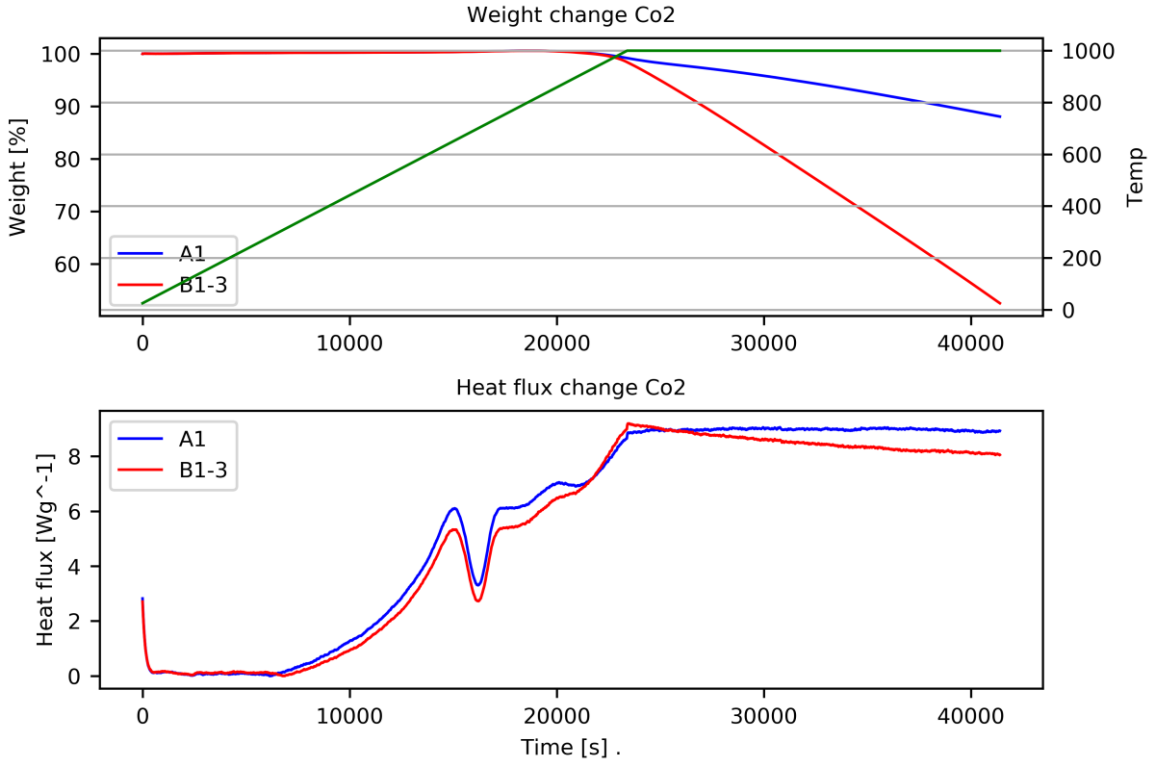

Figure 32 Type A1 and B1-3 in CO2

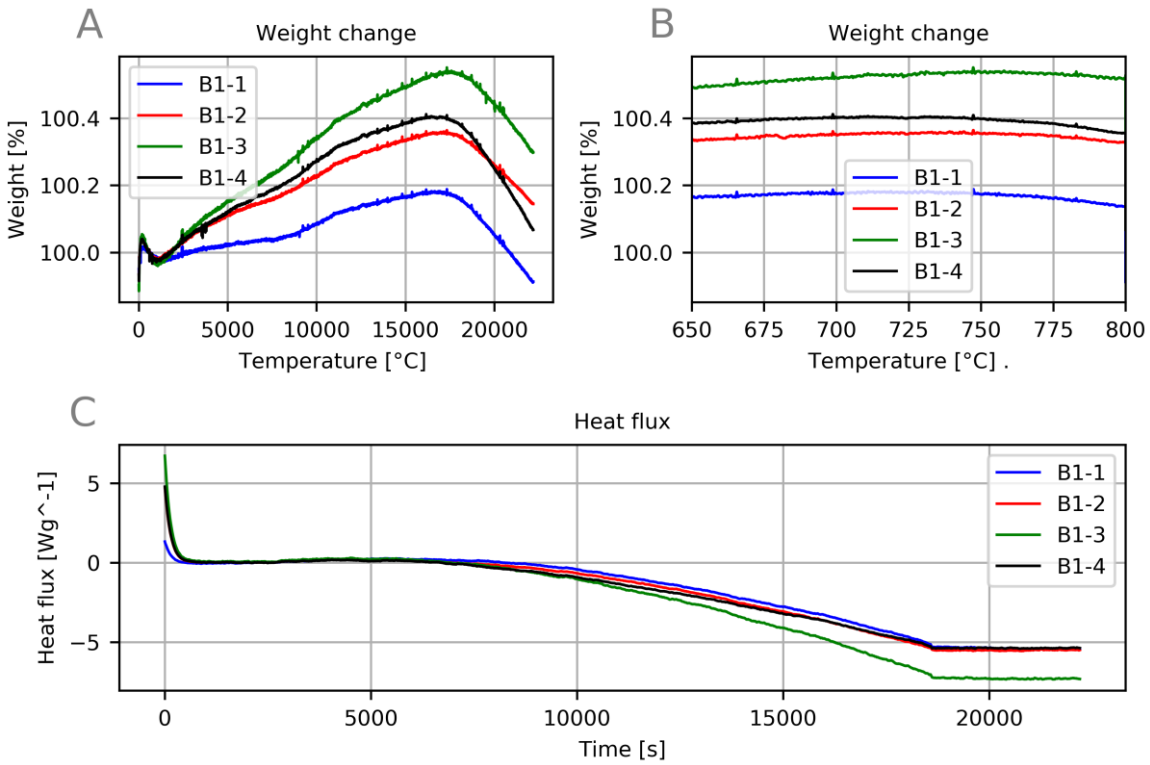

Figure 33 Test of B1-1 to B1-4 in CO2

5.1.4 Step test

The steps test from 640 degrees Celsius to 700 degrees Celsius had to high temperature to help study the coating. The two with lower temperature 500 to 600 and 440 to 500 degrees Celsius test gave some useful results. To show the results, there are used two graphical methods and a table.

In Figure 34 the result of the step test two end three is shown Figure 34 shows the weight loss difference between the two Type A2 coated samples and the reference samples Type A2-Ref . since there is a significant difference, it the A2-2 is also shown in Figure 34C. Fig Figure 34B shows the two B3 coated samples from the step test and their weight loss difference to the reference B3-Ref. In Figure 34D, all the samples are shown, the y-axis is set to 5 to see the B3-coated sample.

The difference in weight per cent at 580-degree Celsius for the Type B coated and Type A coated sample and there respectively reference material is shown in Table 28 where the material resistivity are included. Sample A2-1 has a lower resistivity and a higher weight loss than A2-2. This is also true for B3-3 compared with B3-4. It is important the notice the Type A2-1 and A2-2 coating has a difference in resistivity of 9.9 µΩ*m while B3-3- and B-3-4 has a difference of 309 µΩ*m. This makes it hard to compare the A types and B types of coating together.

There can be seen a flattering between the 560 and 580-degree plot for both A2-2 and B3-3. Those this is not seen in A2-1 and B3-4. The weight difference from the reference at 580-degree Celsius is shown in Table 28

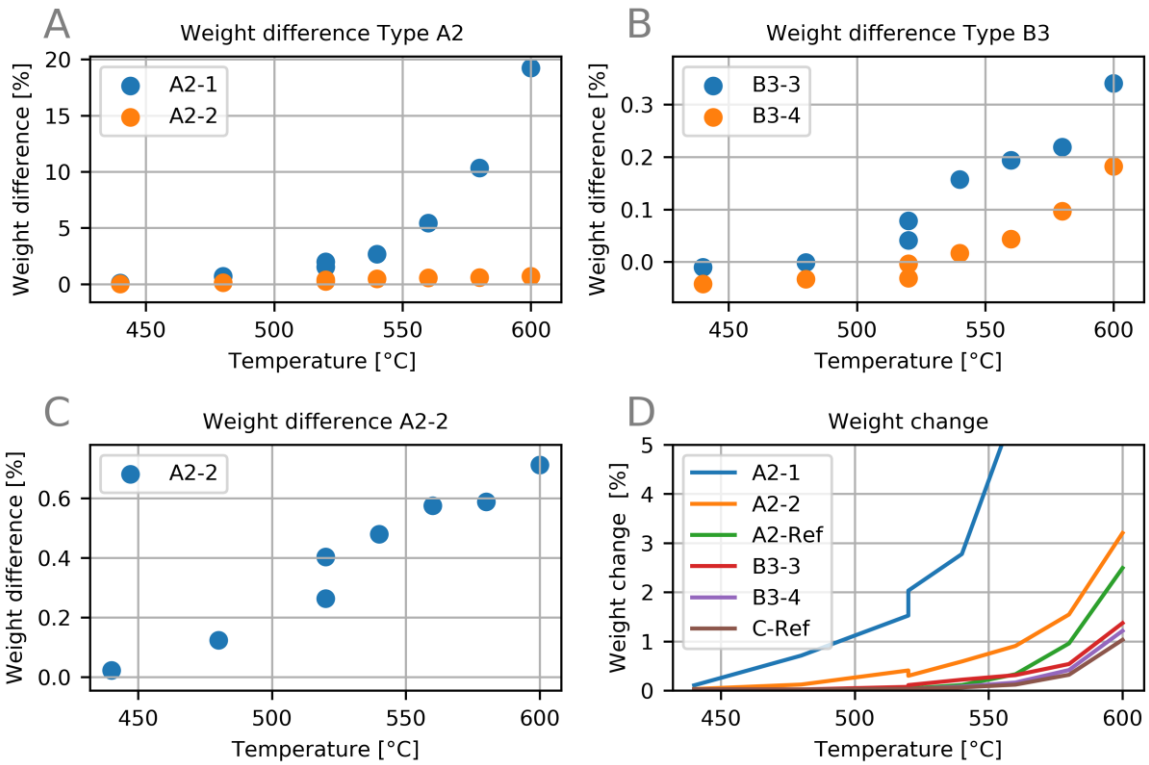

Figure 34 Step test 440-600 degree Celsius, A, B and C is the weight loss difference between the sample and the reference sample. D is the weight loss for the samples.

Table 28 Weight difference at 580 degrees Celsius

Coating Type	A2-1	A2-2	B3-3	B3-4
Weight difference [%]	10.34	0.588	0.2186	0.0967
Resistivity [μΩ*m]	250.8	260.7	441	750

5.2 EIS

There is chosen to focus most on the 80 % SoC when looking at the result because this is a measurement done on all the different cell types, and it is assumed to have less error. Type B had an SoC error that becomes larger at low SoC, and the pat-cell had some error with one cell at 50 % SoC, which has to be seen much time but usually not affected the cell as much as here.

5.2.1 Type A-coating

For the A2 coating, the was four cells, two with coating A2-1 and two with the reference A2-Ref. They are separated into two sets because of the time difference from charge to testing, where set two was tested around three weeks after set one. The plots can be seen in Figure 26. There was also an error at a 50% SoC measurement with a 0.1 voltage amplitude for A2-1- 2. This only affects the 20% SoC measurement.

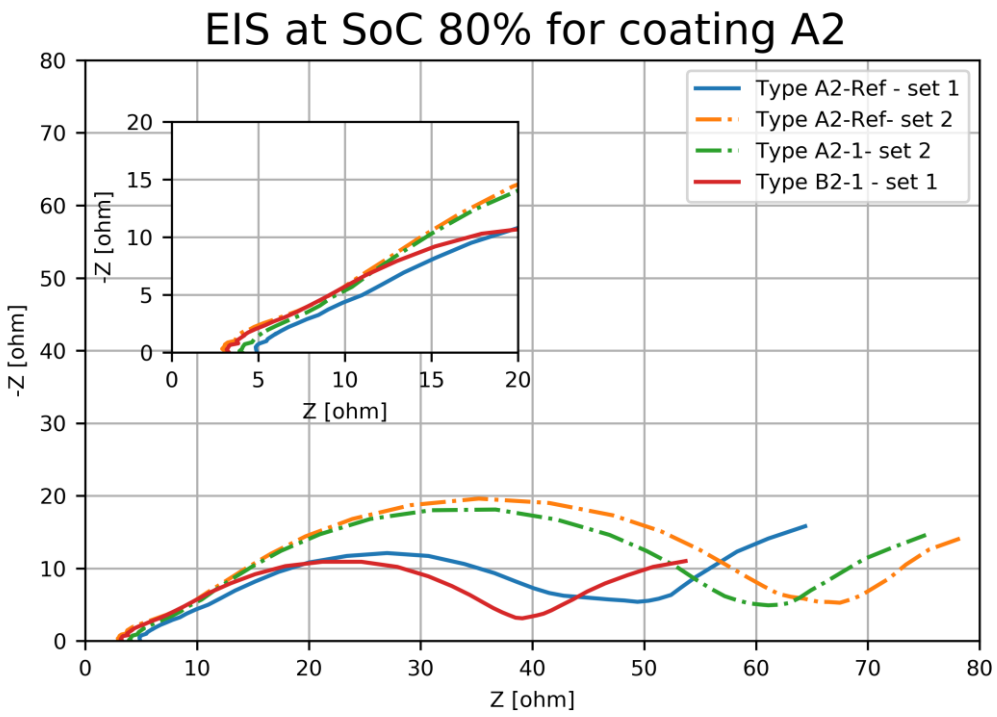

Figure 35 EIS for coating A2 80% SoC

There is a clear difference in the charge transfer between the Type A2-Ref and the Type A2-1. The value is shown in Table 29 The type A2-1 coated sample has 4.14-ohm and 11.6-ohm less charge transfer resistance than the reference.

Table 29 Charge transfers resistant A2.

SoC [%]	Battery			
	Pair one		Pair Two	
	A2-1-1	A2-Ref-1	A2-1-1	A2-Ref-1
20	25.7	34.1	19.2	36.5
50	28.9	26.0	31.7	42.7
80	39.7	21.8	53.4	60.0
Mean	31.4	27.3	34.8	46.4
Difference	41.4		11.6	

5.2.2 Type B-coating

The test of button-cells with coating Type B4 was the first to be done, here the plot of the EIS graph with 0.01 voltage amplitude is shown in Figure 36. There is also zoomed in on the start of the plot. There is a clear difference in the different types. Calculating the slope from the resistivity and charge transfer resistance shows that this increase with a lower SoC %, since the positivity will be the same at all SoC%, but the charge transfer

resistance changes. By instead using the difference in per cent, there is for 50% SoC and 20 % SoC almost no difference.

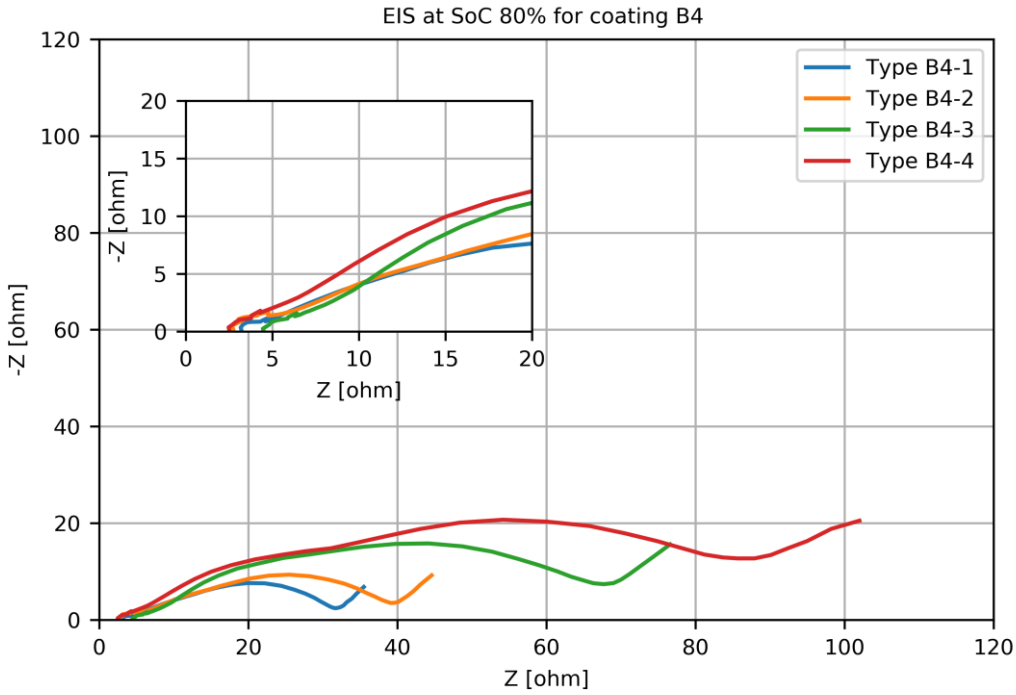

Figure 36 Type B4 coating EIS at 80% SoC

Mulig ikke ta med

Table 30 Type B4 difference in SoC

SoC	Difference between in R_{ct} B4-1 and B4-4 in pro cent [*D*]	Slop R_m/R_{ct}	Slop R_m/D
80%	127	4.71	1.4
50%	87.3	5.82	0.687
20%	87.5	6.17	0.689

Where: R_m = difference in material resistivity
R_{ct} = battery charge transfer resistance

5.2.3 PAT-cells

The Figure 37 shows the 80 % SoC EIS test of the pat-cells with coating type B3, where B3-3 have a smaller charge transfer resistance than the reference sample B3-Ref.

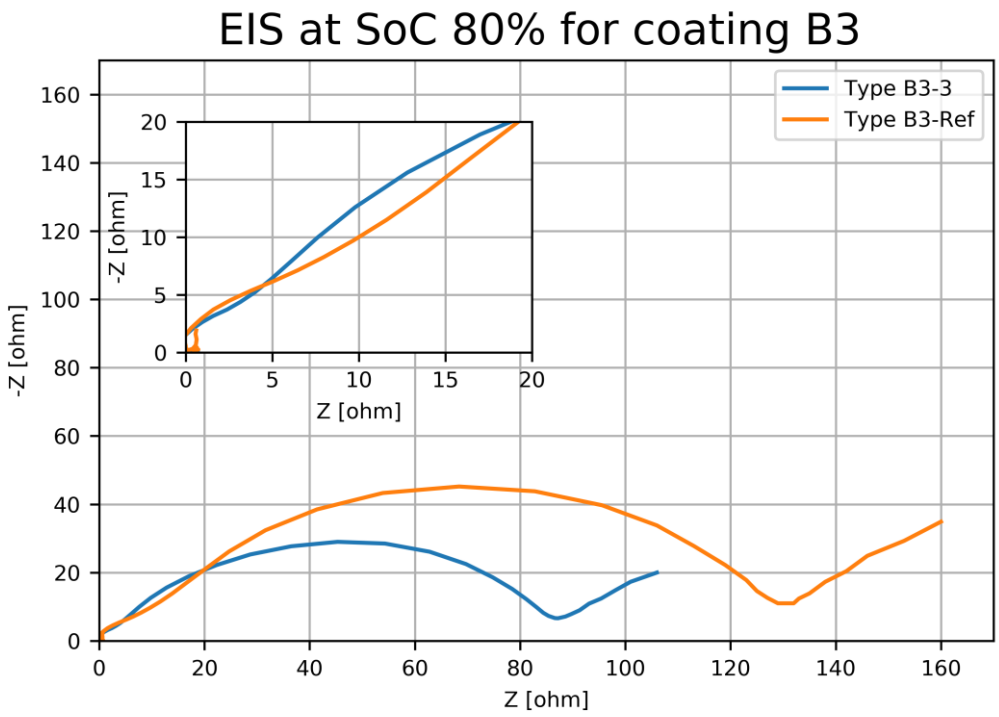

Figure 37 EIS at 80 % SoC for Type B3

5.2.4 Summary

There is a big difference between the coating types of the batteries, but all show the same trend. The more resistivity the material has, the more charge transfer resistance is measured in the EIA measurement, within the same coating Type. Shown in Figure 38. The difference can also be seen by look at the slop in Table 31

Table 31 Slop of the A2, B4 and B3

Coating	Slop 80 % SoC
A2 set 1	12.665
A2 set 2	10.809
B4	4.71
B3	24.528

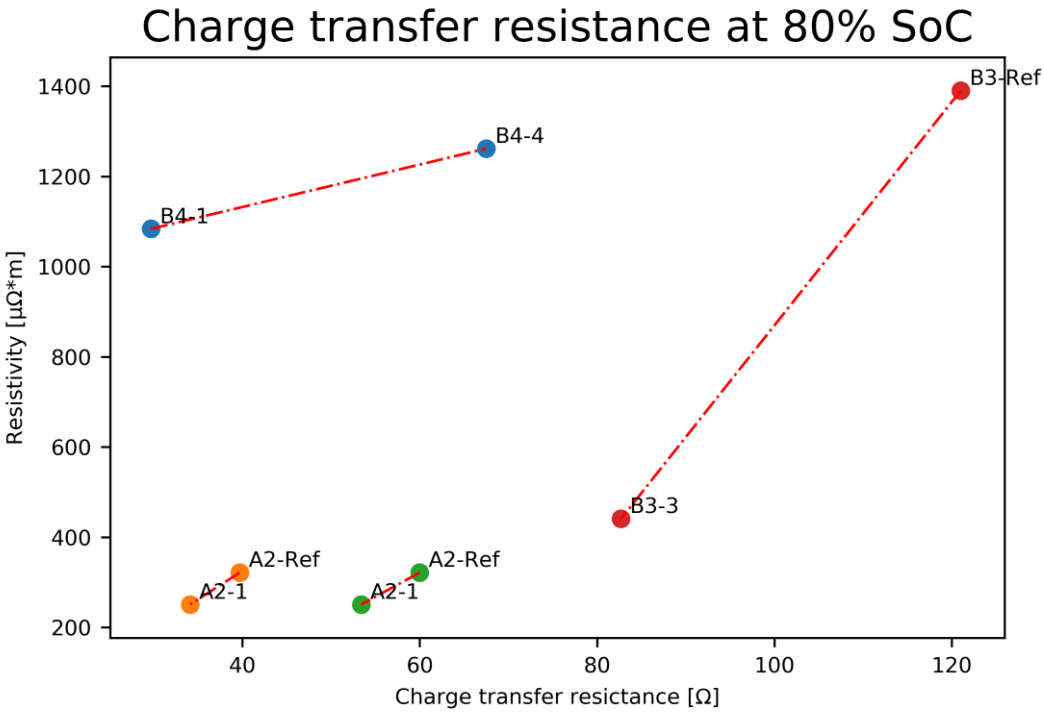

Figure 38 the different cells at 80 % SoC form same set has a line connecting them. The A2-1 and A2-ref is from the same set but done with a 3 weeks time difference.

6 Discussion

6.1 TGA

6.1.1 Flow test

The flow test clearly indicates where the weight change happens. Both, for the coating and the graphite. Thus, it is important to remember that sample A1 has much more coating than the others. The gas flows, 30 mL/min and 50 mL/min, perform alike, but the 60 mL/min shows a slightly higher oxidation rate, i.e. the oxidation proceeds faster at higher air flow which is natural.

It is also possible to see a jump in the heat flux between 10000 and 15000 seconds indicating a downward trend in Figure 23C . The same jump has already been used by Park, Yoon TaeKyu Hong, YoungLee, Ki Tae [16] to identify the weight loss, but it has come on an earlier time before the heat flux in an upward trend, and therefore looks some different. It is, therefore, not so easy to see the actual area of the peak, but easy to see the point where it is at 60 and 50 mL/min flow rate. Thus, it the peak nearly disappeared at 30 mL/min flow, and this flow rate would be a disadvantage with use of this method.

6.1.2 Oxygen tests

All oxygen test are done under an oxygen gas flow rate of 50 mL/min and a heat rate of 2.5 °C/min to study the oxidation profile of the different coating types. From the test of coating Type A2, there can be seen a clear difference between the samples and their weight drop where A2-1 is oxidising at a considerably lower temperature, even though there is a resistivity difference of only 9.9 [μΩ*m] between A2-1 and A2-2. Thus, it is not possible to see separate oxidation of the coating. There are done two tests, and they are very alike and follows a pattern with a higher temperature for the samples with high material resistivity that again indicates a low amount of coating. There is no linear connection between the resistivity and the temperature difference for the weight loss. Unfortunately, there has not been the opportunity to do tests for different samples with Type A coating.

By comparing the A1 and A2-Ref, it is possible to see a clear weight loss and that stabilise before the rest of the sample oxidise. This makes it possible to measure the loss directly without resistivity of the material. However, it also indicates that this is impossible for the other samples, at least to the same degree. They do not have two separate weight drops. There can be a slight weight drop over from two hundred to four hundred degrees Celsius, as is used in - Guo al et." [17], reviewed in the theory chapter.

The quartz sample shows a clear weight drop between 550 and 575 degrees Celsius. Since the sample is coated with quartz, there should not be anything but the coating that can oxidize. Thus, the drop is tiny, around 0.05% and indicate a meagre amount of coating. There is a total weight loss of, 0.15 % to which degree it is volatile from the coating that also causes this is unsure. The temperature coincides with the result in the paper from Park, Yoon Tae, Kyu Hong, YoungLee, Ki Tae [16] mentioned in the theory chapter. This gives a confirmation that this is a temperature area of interest when studying the coating Type B as well as Type A shown in the flow test.

The test of B3 samples does not show a clear connection between the loss temperature and resistivity at 50 % weight loss. There is not any clear trend when extracting the weight at 500 or 580 degrees either. This method was used by - Guo al et."[19]. Where it was a clear difference. However, some of the samples have a higher weight than the reference here. This can be because of noises since there are such small values that are looking at. Thus, for the B3-3 sample, there is a loss for 580 it is larger than with the step test, but only around 25 %, it is still too uncertain to conclude with anything certainly when the other tests do not show the same trend.

Since these two methods did not show a certain result. It was looked at the connection between temperature where a low weight fall had happened and the resistivity. This shows a clear connection.

6.1.3 Carbon dioxide tests

Since the result of the carbon dioxide did not seem to give much information about the coating or follow a pattern, at least without running a very time-consuming test, this was not followed further. However, with more time, tests with CO2 can be a way to determine the amount of coating. There is a clear difference between the A and B types of coating and the rate of weight loss at the isotherm stage of 1000 degree Celsius. This can be caused by different heating of the material in the coating methods.

6.1.4 Step test

In the step test, it was wanted to isolate the weight change from coating oxidation by having isotherm stages where the reaction is assumed to start. The temperature was chosen based on the earlier tests oxidation profiles, especially the quartz test, and the test of coating type A.

For type A coating, there is a significant difference between the two samples A2-1 and A2-2. It is clear that the base material for A2-1 Type coating also oxidates at a lower temperature than for the A2-2 coating. There is more moderate oxidation, but there is still no linear point in the difference between the A2-2 and A2-Ref. Compared with the result for A2-1 and A2-2 in the oxygen at 580 degrees Celsius, the weight loss is larger in the step test. This can indicate that its oxidation process is slow and need a long time the happen.

The two different coatings samples, B3-3 and B3-4, follow each other closely for the type B coating. There is still no point where the difference between the B3-Ref and the two other samples is linear. However, the B3-3 and B3-4 samples have a steady difference between each other from 550 degrees Celsius and up to 600-degree Celsius where the test end. By looking at the oxygen test of the same samples, until 550-degree Celsius, the samples keep a relatively flat weight curve, and this can be a point where it is suitable to look at the weight difference from the reference. This can maybe tell more about the weight difference between the samples Type B3-3 and B3-4, then between them and the B3-Ref.

There is still for both types a connection between resistivity and the weight loss difference from the reference. However, this does not correlate between the Type A and Type B coating, where A has around 20 % with a difference for resistivity difference of 10 [μΩ*m].

In comparison, Type B has 0.15 % weight difference for resistivity of difference of 300 [μΩ*m].

6.2 EIS

6.2.1 Type A-coating

Even though there is a clear difference between the two types of samples, it is not clear when all four cells are compared. The two first cells, A2-1-1 and A2-Ref-1, were tested only a few days after charged. However, the next pair, A2-1-2 and A2-Ref-2, were measured three weeks after charging. The storage time of the cells at relatively high SOC could influence the results significantly as side reactions (electrolyte decomposition) at the anode side could cause an increase in resistance. Cell A2-Ref-2 did have an error when measuring EIS at 50 % SoC, and after the error, there was a clear decline in the cells impedance. For the different pair of batteries tested at the same time, there can be seen the same pattern as mentioned in [Wang et al. – 2013] discussed in the literature review. Because of the time difference and the error in one cell, the first pair of cells should be emphasised.

6.2.2 Type B-coating

There was unfortunately only possible to get the material resistivity for two of the coating types used here. Those two did follow a clear trend between the charge transfer resistance and the material resistivity, Where a lower material resistivity gives a lower charge transfer resistance. The same trend was seen at all three SoC% levels. The connection between the resistivity and the charge transfer resistance changes with different SoC. Since the charge transfer resistance gets smaller at lower SoC, but the material resistivity is the same. This is important to have in mind when using the charge transfer resistance to calculate the amount of coating that the EIS must be done at the same SoC.

6.2.3 PAT-cell

The PAT-cell test looks much like the other, with a lower charger transfer resistance for the coated material. Because of the inconvenience with transport from Elkem and limited time, only 92% and 80% SoC was tested, and only 80% is looked at in the results. One point of interest is that the internal resistant part is almost zero. This is probably because there is less loss when the cell is in a PAT-cell holder.

6.2.4 Summary

From the plot in Figure 38, all the different types of materials follow a trend where higher resistivity gives more charge transfer resistance. From Table 30, the difference in the slope is significant, and it is not possible to give a common equation to calculate the resistivity from the charge transfer with this data. Even when looking at the same type of coating, there is a big difference. Furthermore, by looking at the difference of the A2, it can be seen like time from the charge/ discharge has a lot to say. There are also too few different coatings used to really be able to quantify the relationship between the coating and resistivity.

7 Conclusion

The goal of this thesis was to develop a method to characterize the amount of coating on graphite with the use of TGA and EIS. This included the use of materials resistivity to find a connection between weight loss and resistivity of the different samples. And between the charge transfer resistance and the resistivity of the coated graphite used as an anode. To achieve this, a series of experiments were performed. The result of each experience, supplemented information from the literature, was used to determine the next experiments parameter.

The method developed for investigating the amount of coating on graphite gives good relative results. It is clear that samples with low resistivity have a higher weight loss at 500 to 580-degree Celsius. There has also been possible to approximate the absolute amount of coating on samples with a very tiny coating layer, less than one weight per cent. By slowly oxidising the samples at a given temperature and compared them with an uncoated reference sample. For higher amounts of coating 1-2 weight per cent and more, and coating that oxidising easy, the weight can be measured by isoconversion burning at a constant heat rate where two different peaks are seen. It was also found a connection between the resistivity and the main weight fall temperature on some coating groups.
The method with use of EIS to find the charge transfer resistance and look at the relationship between the charge transfer and the resistivity of the material used in the anode did show a clear connection in all the tested samples. It can also be seen that there is a large difference between the main Type of coating A and B.

For both methods, TGA and EIS, there are too few samples to conclude which approach work best to estimate the amount of coating. The difference in the type of coating also opens the possibility that different approaches should be used at the different coating types. It is not focused as much on the thickness of the coating. To be able to measure the weight, is the first step to find the thickness. With little information to control the result and few samples, it was more befitting to prioritise the method for finding the weight loss.

8 Recommendations

Finding the thickness of the coating with the help of the weight or in another way directly from TGA or EIS experiment and resistivity can be an interesting extension of the work. The method should also be further tested. With more samples and addental control of the coating weight, it would then maybe be possible to develop an equation that can tell the weight or thickness of the coating only from the material resistivity. If the is much data about earlier tests of coating and its weight, it could also be an idea to use machine learning to characterize the coating

List of References

[1] B. Scrosati, "History of lithium batteries," *J. Solid State Electrochem.*, vol. 15, no. 7–8, pp. 1623–1630, 2011, doi: 10.1007/s10008-011-1386-8.
[2] Isidor Buchmann, "BU-301a: Types of Battery Cells." https://batteryuniversity.com/learn/article/types_of_battery_cells.
[3] C. Daniel and J. O. Besenhard, *Handbook of Battery Materials Second, Completely Revised and Enlarged Edition*. 2011.
[4] M. Danko, J. Adamec, M. Taraba, and P. Drgona, "Overview of batteries State of Charge estimation methods," *Transp. Res. Procedia*, vol. 40, pp. 186–192, 2019, doi: 10.1016/j.trpro.2019.07.029.
[5] N. Nitta, F. Wu, J. T. Lee, and G. Yushin, "Li-ion battery materials: Present and future," *Mater. Today*, vol. 18, no. 5, pp. 252–264, 2015, doi: 10.1016/j.mattod.2014.10.040.
[6] D. Deng, "Li-ion batteries: Basics, progress, and challenges," *Energy Sci. Eng.*, vol. 3, no. 5, pp. 385–418, 2015, doi: 10.1002/ese3.95.
[7] N. Mohamed and N. K. Allam, "Recent advances in the design of cathode materials for Li-ion batteries," *RSC Adv.*, vol. 10, no. 37, pp. 21662–21685, 2020, doi: 10.1039/d0ra03314f.
[8] Energizer Holdings, "Battery internal resistance," *Pulse*, no. December, pp. 1–2, 2005, [Online]. Available: http://data.energizer.com/pdfs/batteryir.pdf.
[9] H. G. Schweiger *et al.*, "Comparison of several methods for determining the internal resistance of lithium ion cells," *Sensors*, vol. 10, no. 6, pp. 5604–5625, 2010, doi: 10.3390/s100605604.
[10] R. Korthauer, *Lithium-ion batteries: Basics and applications*. 2018.
[11] H. O. Pierson, "Handbook of carbon, graphite, diamond and fullerenes, Noyes publications," *Noyes, Park Ridge, NJ*, p. 398, 1993.
[12] S. Nasir, M. Z. Hussein, Z. Zainal, and N. A. Yusof, "Carbon-based nanomaterials/allotropes: A glimpse of their synthesis, properties and some applications," *Materials (Basel).*, vol. 11, no. 2, pp. 1–24, 2018, doi: 10.3390/ma11020295.
[13] H. Marsh, *Introduction to Carbon Science*, 1. Butterworth & Co., 1989.
[14] N. A. Kaskhedikar and J. Maier, "Lithium storage in carbon nanostructures," *Adv. Mater.*, vol. 21, no. 25–26, pp. 2664–2680, 2009, doi: 10.1002/adma.200901079.
[15] J. Asenbauer, T. Eisenmann, M. Kuenzel, A. Kazzazi, Z. Chen, and D. Bresser, "The success story of graphite as a lithium-ion anode material-fundamentals, remaining challenges, and recent developments including silicon (oxide) composites," *Sustain. Energy Fuels*, vol. 4, no. 11, pp. 5387–5416, 2020, doi: 10.1039/d0se00175a.
[16] P. Kurzweil and K. Brandt, *Overview of rechargeable lithium battery systems*. Elsevier B.V., 2018.
[17] A. Mauger and C. Julien, "Surface modifications of electrode materials for lithium-ion batteries: Status and trends," *Ionics (Kiel).*, vol. 20, no. 6, pp. 751–787, 2014, doi: 10.1007/s11581-014-1131-2.
[18] Y. T. Park, Y. Kyu Hong, and K. T. Lee, "Effect of amorphous carbon coating on low-purity natural graphite as an anode active material for lithium-ion batteries," *J. Ceram. Process. Res.*, vol. 18, no. 7, pp. 488–493, 2017.
[19] R. Guo, P. Shi, X. Cheng, and C. Du, "Synthesis and characterization of carbon-coated LiNi1/3Co1/3Mn1/3O2 cathode material prepared by polyvinyl alcohol

pyrolysis route," *J. Alloys Compd.*, vol. 473, no. 1–2, pp. 53–59, 2009, doi: 10.1016/j.jallcom.2008.05.102.
[20] A. Celzard, J. F. Marêché, F. Payot, and G. Furdin, "Electrical conductivity of carbonaceous powders," *Carbon N. Y.*, vol. 40, no. 15, pp. 2801–2815, 2002, doi: 10.1016/S0008-6223(02)00196-3.
[21] W. Choi, H. C. Shin, J. M. Kim, J. Y. Choi, and W. S. Yoon, "Modeling and applications of electrochemical impedance spectroscopy (Eis) for lithium-ion batteries," *J. Electrochem. Sci. Technol.*, vol. 11, no. 1, pp. 1–13, 2020, doi: 10.33961/jecst.2019.00528.
[22] A. Lasia, *Electrochemical Impedance Spectroscopy and its Applications*. 2014.
[23] S. S. Zhang, K. Xu, and T. R. Jow, "EIS study on the formation of solid electrolyte interface in Li-ion battery," *Electrochim. Acta*, vol. 51, no. 8–9, pp. 1636–1640, 2006, doi: 10.1016/j.electacta.2005.02.137.
[24] Y. Tian, Z. Sun, Y. Zhang, X. Wang, Z. Bakenov, and F. Yin, "Micro-spherical sulfur/graphene oxide composite via spray drying for high performance lithium sulfur batteries," *Nanomaterials*, vol. 8, no. 1, 2018, doi: 10.3390/nano8010050.
[25] C. Wang, H. Zhao, J. Wang, J. Wang, and P. Lv, "Electrochemical performance of modified artificial graphite as anode material for lithium ion batteries," *Ionics (Kiel).*, vol. 19, no. 2, pp. 221–226, 2013, doi: 10.1007/s11581-012-0733-9.